Crystal Structure Transformations in Inorganic Nitrites, Nitrates, and Carbonates

C. N. R. Rao, B. Prakash, and M. Natarajan

Department of Chemistry,
Indian Institute of Technology,
Kanpur, India

U.S. DEPARTMENT OF COMMERCE, Rogers C. B. Morton, *Secretary*
NATIONAL BUREAU OF STANDARDS, Richard W. Roberts, *Director*

Issued May 1975

Library of Congress Cataloging in Publication Data

Rao, Chintamani Nagesa Ramachandra.
Crystal structure transformations in inorganic nitrites, nitrates, and carbonates.

(NSRDS-NBS 53)
Supt. of Docs. no.: C 13.48.53
1. Crystals. 2. Phase rule and equilibrium.
I. Prakash, Brahm, 1912- joint author.
II. Natarajan, M., joint author. III. Title.
IV. Series: United States. National Bureau of Standards. National Standard Reference Data Series, NSRDS-NBS 53.
QC100.U573 no. 53 [QD921] 389'.6'08s [548'.81]
74-18389

NSRDS-NBS 53
Nat. Stand. Ref. Data Ser., Nat. Bur. Stand. (U.S.), 53, 48 pages (May 1975)
CODEN: NSRDAP

U.S. GOVERNMENT PRINTING OFFICE
WASHINGTON: 1975

For sale by the Superintendent of Documents, U.S. Government Printing Office, Washington, D.C. 20402
(Order by SD Catalog No. C13.48:53). Price $1.15

Foreword

The National Standard Reference Data System provides access to the quantitative data of physical science, critically evaluated and compiled for convenience and readily accessible through a variety of distribution channels. The System was established in 1963 by action of the President's Office of Science and Technology and the Federal Council for Science and Technology, and responsibility to administer it was assigned to the National Bureau of Standards.

NSRDS receives advice and planning assistance from a Review Committee of the National Research Council of the National Academy of Sciences-National Academy of Engineering. A number of Advisory Panels, each concerned with a single technical area, meet regularly to examine major portions of the program, assign relative priorities, and identify specific key problems in need of further attention. For selected specific topics, the Advisory Panels sponsor subpanels which make detailed studies of users' needs, the present state of knowledge, and existing data resources as a basis for recommending one or more data compilation activities. This assembly of advisory services contributes greatly to the guidance of NSRDS activities.

The System now includes a complex of data centers and other activities in academic institutions and other laboratories. Components of the NSRDS produce compilations of critically evaluated data, reviews of the state of quantitative knowledge in specialized areas, and computations of useful functions derived from standard reference data. The centers and projects also establish criteria for evaluation and compilation of data and recommend improvements in experimental techniques. They are normally associated with research in the relevant field.

The technical scope of NSRDS is indicated by the categories of projects active or being planned: nuclear properties, atomic and molecular properties, solid state properties, thermodynamic and transport properties, chemical kinetics, and colloid and surface properties.

Reliable data on the properties of matter and materials is a major foundation of scientific and technical progress. Such important activities as basic scientific research, industrial quality control, development of new materials for building and other technologies, measuring and correcting environmental pollution depend on quality reference data. In NSRDS, the Bureau's responsibility to support American science, industry, and commerce is vitally fulfilled.

RICHARD W. ROBERTS, *Director*

Preface

Many inorganic solids undergo transformations from one crystal structure to another. Studies of these phase transformations are of value in understanding the nature and properties of solids. Recent literature abounds with information on phase transformations of solids and it is often difficult to obtain relevant data or references on the transformation(s) of any specific substance. We, therefore, considered it worthwhile to collect the literature on the phase transformations of various types of inorganic solids and present them in an organized manner. As part of this program, we published monographs on binary halides (NSRDS–NBS–41) and transition metal oxides (NSRDS–NBS–49) some time ago. In this monograph, we have reviewed the important data on the crystal structure transformations of salts of three typical oxyanions, nitrites, nitrates and carbonates. These salts exhibit several types of interesting transformations which have been examined by a variety of techniques. We plan to publish reviews on inorganic sulfates and other solids in the future.

In preparing this monograph, we have surveyed most of the material abstracted up to June 1973 in Chemical Abstracts. We have listed the important references to the published literature after presenting the survey on each solid. In reporting the information on the transformations of a solid, we have indicated the methods employed as well as the important data and conclusions. For each solid, we have given the crystallographic data for the stable phase around room temperature and at atmospheric pressure, making use of the standard data published by NBS whenever possible.

We are thankful to Mr. S. Chattopadhyay for his assistance in the literature survey.

Contents

	Page
Preface	IV
Introduction	1
Units, Symbols and Abbreviations	2
1. Nitrites	2
1.1. Alkali metal nitrites	2
1.2. Alkaline earth metal nitrites	9
1.3. Thallium nitrite	10
2. Nitrates	10
2.1. Nitric acid	10
2.2. Alkali metal nitrates	10
2.3. Ammonium nitrate	24
2.4. Thallous nitrate	30
2.5. 3*d* Transition metal nitrates	33
2.6. Silver nitrate	35
3. Carbonates	37
3.1. Alkali metal carbonates	37
3.2. Alkaline earth metal carbonates	38
3.3. Thallous carbonate	45
3.4. 3*d* Transition metal carbonates	46
3.5. Silver carbonate	48

[5] Stern, K. H., and Weise, E. L., High Temperature Properties and Decomposition of Inorganic Salts, Part 2, Carbonates, NSRDS-NBS-30, National Bureau of Standards, November 1969.
[6] Stern, K. H., High Temperature Properties and Decomposition of Inorganic Salts, Part 3, Nitrates and Nitrites, J. Phys. Chem. Ref. Data, **1**, 747–772, 1972.

Units, Symbols, and Abbreviations

P = Pressure; 1 atm., (~ 1 bar) = 101325 Nm^{-2} = 1013250 dyn cm^{-2}
T = Temperature in kelvins
R = Gas constant = 8.3143 J mol^{-1} deg^{-1} = 1.98717 cal mol^{-1} deg^{-1}
J = Joule
C = Coulomb
Hz = Hertz (cycle/second)
V = Volt
cal = Thermochemical calorie = 4.1840 J
T_t = Transformation temperature
ΔT = Thermal hysteresis in a reversible transformation
ΔH_{tr} = Enthalpy change accompanying the transformation
ΔS_{tr} = Entropy change accompanying the transformation
ΔV = Entropy change accompanying the transformation
T_c = Curie Temperature
T_N = Néel temperature
C_p = Heat capacity at constant pressure
C_m = Magnetic heat capacity
σ = Electrical conductivity
ρ = Density (in grams per cm^3)
ϵ = Dielectric constant
tan δ = Dissipation factor
P_s = Spontaneous polarization
E_c = Coercive field
E_a = Energy of activation
ΔG = Gibb's free energy change
χ = Magnetic susceptibility
τ = Relaxation time
Z = Number of molecules per unit cell
IR = Infrared
UV = Ultraviolet
DTA = Differential thermal analysis
NMR = Nuclear magnetic resonance
NQR = Nuclear quadrupole resonance
ESR = Electron spin resonance.

1. Nitrites

The nitrites of only the alkali metals (especially Na and K) have been extensively studied and these undergo phase transformations. The following is an account of the available information regarding the phase transitions of inorganic nitrites.

1.1. Alkali Metal Nitrites

The transformation temperature, melting point, dissociation point, and the heat of transition of alkali metal nitrites are given below [1–3]:

Transitions in alkali metal nitrites

	T_t, K	Melting point, K	Dissociation point, K	ΔH_{tr}, cal mol^{-1}
$LiNO_2$.....	367	493	503	—
$NaNO_2$.....	439	555	703	250
KNO_2	320	711	753	120 ± 30
$RbNO_2$.....	348	695	793	500 ± 50
$CsNO_2$.....	393	673	783	1100 ± 100

The transformation temperature, T_t, does not show any systematic trend. The transformations in $LiNO_2$, $RbNO_2$, and $CsNO_2$ have not been studied in detail, but a number of workers have investigated the transformation in $NaNO_2$ and KNO_2 by a variety of techniques.

Lithium Nitrite, $LiNO_2$ (No crystal data seem to be available).

Protsenko and coworkers [3] have reported a phase transformation in lithium nitrite at 367 K. The transformation has been characterized by the anomaly in the DTA and electrical conductivity measurements.

Sodium Nitrite, $NaNO_2$, orthorhombic (body-centered), C_{2v}^{20}-Im2m, $z = 2$, $a = 3.570$ Å, $b = 5.578$ Å, $c = 5.390$ Å at 299 K.

Sodium nitrite was found to be ferroelectric a number of years after the discovery of its phase transition and the literature on the ferroelectric transition of $NaNO_2$ up to 1962 has been reviewed by Jona and Shirane [3a]. Ferroelectricity in this compound was predicted by Zheludev and Sonin [4] in 1957 from the changes in point group symmetry due to the ferroelectric phase transition and was independently observed by Sawada et al. [5]. During the past decade, this solid has attracted considerable attention which has led to numerous investigations of its various physical properties such as dielectric constant [6–10], domain structure [11–13], specific heat [14–16], thermal expansion [14, 16–18], thermal conductivity [19], electrical resistivity [20], NMR [21], x-ray diffraction [12, 17, 22, 23], and optical properties [24–27].

Sodium nitrite at normal temperature and pressure has a body-centered orthorhombic unit cell. It is ferroelectric with the spontaneous polarization parallel to the *b*-axis and undergoes a first order transformation to the paraelectric phase around 438 K. Between the ferroelectric (III) and paraelectric (I) phases, a sinusoidal antiferroelectric phase (II) has been reported to exist over the narrow temperature range of 436.8–438 K [10, 10a, 15, 16, 18, 21, 28].

In the ferroelectric phase, the NO_2^- ions are parallel in the *a*-planes; the ordering parameter of the NO_2^- ions in the *a*-plane changes sinusoidally along the *a*-axis with a period of about eight layers [28]. Sawada et al. [29] have studied the domain reversal of $NaNO_2$ and discussed the "Himidashi" (bulging out) phenomenon peculiar to this solid caused by the variation of spontaneous polarization (P_s) and the coercive field (E_c) with the size of the electrode. Recently, Flügge and Meyenn [29a] have studied the theoretical aspects of the order disorder transition in $NaNO_2$ in which a two sublattice model of interacting dipoles is treated in a molecular field approximation to describe the ferro- and paraelectric properties of $NaNO_2$. Polarization values thus calculated, are found to be in good agreement with experiment for the narrow antiferroelectric domain not resolved by the model. Yamada and Yamada [29b] had pointed out earlier that the long-range, dipole-dipole type interaction plays the important role to initiate the phase transitions in sodium nitrite.

In addition to the transitions, III → II and II → I, some anomalies at 375, 451, and 488 K have also been reported [17, 18, 30]. These anomalies are believed to be related to anisotropic vibrorotatory states of the NO_2^- ions.

Gesi [31] has reported a new phase transformation (III–IV) in ferroelectric $NaNO_2$ at 178 K from precise measurements of thermal expansion and low frequency dielectric constant at normal pressure. Phase IV is a high pressure phase existing at 8 kbar and room temperature and is described in detail later in this section. This III–IV transition did not show any thermal hysteresis and is of second order since no discontinuous change was found either in dielectric constant or volume thermal expansion measurements.

High Pressure Transformations: Bridgman [32] detected a high pressure transition, probably of the second order, as a break in the slope of the compression curve of the solid. This transition was also observed optically by Lippincott et al. [33] in their high pressure anvil device. They measured the bending vibration frequency ν_2 of NO_2^- in $NaNO_2$ at high pressure and found an abrupt change in ν_2 from 825 cm^{-1} at atmospheric pressure to 855 cm^{-1} after the III–IV transition at 14.5 kbar. This indicates a change in the electronic structure (or the shape of the NO_2^- ion) during the III–IV transition. Rapoport [34] has determined the phase diagram of $NaNO_2$ up to 40 kbar and from room temperature to 773 K. The phase diagram consists of five solid phases abbreviated as I, II, III, IV, and V. The I, II, and III phases are the paraelectric, antiferroelectric, and ferroelectric phases, respectively. Phase IV is identical to the high pressure phase described by Bridgman [32] and is the same found by Gesi [31] below 178 K. Phase V is another high pressure phase which exists just below the melting point above 10 kbar. Rapoport has indicated that the extrapolation of III–IV phase boundary to atmospheric pressure gives a temperature of 168 K. The problem whether the room-temperature phase III transforms to the high pressure phase IV at atmospheric pressure or not is interesting. The ferroelectric Curie point, T_c, (III–II phase transition) and the Neel point, T_N (I–II phase transition) were detected by DTA up to 40 kbar. These results were found to agree well with those of Gesi [31].

Measurement technique	Observations	Remarks	References
X-ray diffraction	T_t, 436 K	Ferroelectric $NaNO_2$ crystal transforms through the first order transition to an antiferroelectric phase with a sinusoidal modulation of the moment in which the antiferroelectric order is partially attained. The system transforms to a paraelectric phase at a higher temperature. The successive appearance of these phases, the order of transition, the temperature dependence of the order parameter and the anomalous volume expansion are explained by a thermodynamic calculation on the basis of a molecular field approximation.	[28].
X-ray investigation of the disordered structure of $NaNO_2$ near T_c (~ 433 K).		The observed diffuse scattering, the satellites and the plate-like diffuse scattering normal to the b-axis around them can be interpreted on the basis of a disordered arrangement of two kinds of structural units. The atomic positions in each structural unit were determined from the relative intensity of the Bragg reflections and that of the satellites.	[23, 35].
		The structure factors and the corresponding Fourier synthesis were also calculated. It is concluded that at 423 K, about 15 percent of the NO_2 groups are in their centrosymmetric positions.	[36].
Differential Thermal Analysis	T_t, 433–435 K		[37].
Differential scanning calorimetry.	Enthalpy of phase transition, ΔH_{tr}, 299 ± 33 cal mol^{-1}.		[38].
Specific heat measurements in an adiabatic calorimeter.	The specific heat starts to increase anomalously at 373 K. At 436 K, there is a sharp peak in the curve. At 437 K a small peak appears after which the specific heat decreases gradually with increasing temperature up to 453 K.	The first anomaly corresponds to the first order ferroelectric to antiferroelectric phase transition, while the second anomaly is regarded to be due to an antiferroelectric-paraelectric phase transition.	[15].
Thermal conductivity in the range 343–463 K along a, b, and c axes.	Thermal conductivities in the b and a directions show a gradual decrease on heating over a wide temperature range of 50 K below the transition. This decrease is due to an additional thermal resistivity. No anomaly is found in the temperature dependence of thermal conductivity in the c-direction.	A tentative model of the order-disorder arrangement of the NO_2^- ions is proposed to account for the origin of the additive thermal resistivity in which uneven interatomic forces, due to the disordered as scattering centers of phonons.	[19].
Thermal expansion and dielectric studies.	A new phase transformation at 178 K in $NaNO_2$ (ferroelectric phase) is indicated by slight break in these properties both in dielectric constant *versus* temp. and thermal expansion *versus* temperature curves.	The transition is believed to be the III–IV transition in which the ferroelectric $NaNO_2$ transforms to the high pressure phase which exists above 8 kbar at 298 K.	[31].

$NaNO_2$ – Continued

Measurement technique	Observations	Remarks	References
Dielectric Studies, in dc bias fields up to 3.5 kV cm^{-1} at 436–437 K.	The temperature range studied is between T_c (Curie Temperature) and T_N (Neel Temperature).	It is difficult to conclude whether the ferroelectric phase to sinusoidal phase transition becomes first order with increasing bias fields. The sinusoidal state narrows gradually and disappears at ~ 2.6 kV cm^{-1}.	[39].
Dielectric and pyroelectric measurements (ϵ measured along the ferroelectric b axis.	ϵ_b shows a distinct anomaly at T_c and obeys Curie-Weiss law, below and above T_c. The ratio of the Curie constants was found to be 9.6 : 1.	.....	[6].
Experimental (dielectric constant, pyroelectric current etc) and theoretical studies.	ϵ shows a peak at 437.2 K while heating and 435.6 K while cooling. Dielectric dispersion exists in all axial directions $P_s \sim 8.6$ μC cm^{-2} estimated from pyroelectric current measurements, at room temperature.	Ferroelectricity in $NaNO_2$ is discussed phenomenologically taking account of the electrocaloric effect. It is concluded that the transition in $NaNO_2$ is a first order one and that the main contribution to the spontaneous polarization comes from the relative displacement between Na^+ and NO_2^- ions. Also the ferroelectric $NaNO_2$ is half-way between an ionic and a molecular crystal.	[9].
Electrical conductivity (polycrystalline pellet).	The conductivity-temperature curves showed discontinuities or change in slope at or near the transformation temperature.	.....	[40].
Infrared Spectra.....	Transitions are associated with changes in vibration frequency. $NaNO_2$ exhibits changes of all the parameters of the Urbach equation.	Transition in ferroelectric crystals can be correlated with dynamic theories of the crystal lattice of $NaNO_2$.	[41].
Raman Spectra range: 303–451 K.	Raman lines show marked changes near the transition points.	A group theoretical treatment of the vibrational spectrum of the $NaNO_2$ crystal is presented for the low and high temperature modifications of $NaNO_2$.	[42].
Range: 313–493 K.....	The temperature dependence of frequencies of bands at 119, 153, and 220 cm^{-1} shows an abnormal decrease in the frequency of the dipole vibration at 153 cm^{-1}.	The decrease in the dipole vibration frequency has been discussed on the basis of the Ginzburg-Anderson-Cochran theory.	[43].
Range: 323–455 K	Spontaneous polarization disappears above the λ-point.	The disappearance of P_s has been explained partially by reorientation of some NO_2^- groups as a result of their rotation by 180° around the axis parallel to the line joining O-atoms. The forms of normal vibrations are considered on the basis of symmetry coordinates and the intensity of lines. Recent studies [45a], however rule out any major difference between the low and high temperature spectra. It seems that crystal symmetry is not changed during the transformation.	[44, 45].
Ultraviolet Absorption spectra.	A gradual shift of absorption bands is found to accompany thermal expansion of the crystal. An abrupt change in the absorption spectrum is observed at transformation points. $T_t \sim 313$–323 K (II → I) (marked hysteresis).	These two effects of temperature seem to be correlated. In cases where crystal structures are known, shifts in absorption maxima due to changes in temperature have been interpreted in relation to changes in the cation-anion distances.	[26].

$NaNO_2$ – Continued

Measurement technique	Observations	Remarks	References
Neutron diffraction.....	$T_t \sim 438$ K.....	The larger increase in μ_x than in μ_y (μ = root-mean-square amplitude) for the N-atom might indicate the expected rotation about (001). μ of motion for O-atoms are ambiguous.	[46].
Nuclear relaxation.....	A peak is observed in the Na^{23} nuclear relaxation rates, at the ferroelectric transition.	This effect is explained on the basis of the theory of the transition in terms of lattice dynamics. It is argued that nuclear-spin-phonon relaxation can be a powerful tool of investigation for a ferroelectric transition.	[47].
Nuclear quadrupole resonance.	N^{14} NQR lines have been observed in the ferroelectric-phase of $NaNO_2$ and the change of NQR frequencies with τ between 77 and 437 K has been investigated. The NQR frequency seems to begin to deviate from the rigid molecule vibration model around III–IV transition.	The results can be explained by an order-disorder model where the NO_2^- ions are flipping between two equilibrium sites. Disappearance of ferroelectricity can be attributed to the onset of rotation of NO_2^- ions above T_t (473 K).	[48, 49].
Effect of hydrostatic pressure on T_c and T_N up to 10 kbar.	Both T_c and T_N increase with increasing pressure.	The experimental results could be fairly explained on the basis of a phenomenological model developed by Gesi. The model includes a three dimensional lattice strain and accounts for the dielectric constant variation in a bias field.	[50, 51].

Potassium Nitrite, KNO_2, rhombohedral, $R\bar{3}m$, $Z = 1$, $a = 4.455$ Å, $\alpha = 68°58'$ at 298 K (54).

The room-temperature structure of KNO_2 was first considered to have monoclinic symmetry (space group C_s^3-Am) [52], but recent studies [52a–54] have established the structure to be rhombohedral with a centrosymmetric space group $R\bar{3}m$. The unit-cell parameters for a disordered, rhombohedral, room temperature phase according to Solbakk and Strømme [53] are: $a = b = 5.011$ Å, $c = 10.153$ Å with $Z = 3$. The crystal structure of KNO_2 at low temperatures (253 K) has monoclinic symmetry, space group, $P2_1/c$, and the unit cell parameters $a = 4.16 \pm 0.02$ Å, $b = 962 \pm 0.05$ Å, $c = 6.19 \pm 0.03$ Å, $\beta = 113 \pm 1°$, $Z = 4$. Above 313 K, KNO_2 is cubic (Fm3m), with $a = 6.66$ Å, $Z = 4$ at 318 K (53).

Three transformations are known in KNO_2. Denoting the various phases as I, II, and III, the transformations can be described as follows (55):

$$\underset{\text{(monoclinic)}}{\text{III}} \underset{\rightleftharpoons}{\overset{260\text{ K}}{\rightarrow}} \underset{\text{(rhombohedral)}}{\text{II}} \underset{\rightleftharpoons}{\overset{313\text{ K}}{\rightarrow}} \underset{\text{(cubic)}}{\text{I}}$$

Another transition is reported at 343 K by Tanisaki and Ishimatsu [54] who also report an appreciable dielectric anomaly at ~ 230 K. Ray and Ogg [56] report $\Delta H_{tr} \sim 1200 \pm 200$ cal mol^{-1} for the transition at 260 K. The nature of the transition around 313 K has been controversial and was considered to be a ferroelectric-paraelectric transformation by Rao and Rao [57]. Recently, Mansingh, and Smith [55] in their studies of dielectric constant and electrical conductivity have concluded that there is no ferroelectric phase in KNO_2 up to its melting point. At 313 K, there is only a crystal structure change from the rhombohedral to the cubic form. This has also been supported by the assignment of a centrosymmetric ($R\bar{3}m$) space group to KNO_2 by Solbakk and Strømme [53]. Above 319 K, KNO_2 has the cubic NaCl structure with $a = 6.71$ Å [56]. Doucet and coworkers [58] have reported a hitherto unknown transition in KNO_2 at ~ 402 K from x-ray and dielectric constant measurements.

High Pressure Transformations: Bridgman [59] reported a high pressure transition in potassium nitrite. He however, used a rather impure sample (~ 89%

purity). High pressure transitions at 260 K and 320 K have been reported by Ray and Ogg [56] and Hazlewood et al. [60], respectively. A continuous transformation starting at about 638 K has also been observed. Rapoport [34] and Clark and Rapoport [61] showed the phase diagram of KNO_2 to consist of the six solid phases given below:

Phase diagram of KNO_2

Phase	Crystal structure	Range of stability
I.....	Cubic, NaCl type.....	Above 323 K and below 10 kbar.
II.....	Cubic, distorted NaCl type.	Below 323 K and 8 kbar.
III.....	(metastable phase)...	Below 273 K and 8 kbar.
IV.....	Cubic, distorted CsCl type.	Above 273 K and 10 kbar.
V.....	Cubic, CsCl type	Above 345 K and 10 kbar.
VI.....	.....	Around 373 K and ~ 35 kbar.

The I–II and IV–V phase boundaries determined by DTA were found to rise very slowly with pressure. The II–IV, I–IV and I–V boundaries were determined by the volume discontinuity method. In this work two new high pressure phases, V and VI, were discovered. The melting curve of KNO_2 exhibited a maximum at 7.0 kbar and 739 K, and meets the I–V boundary at a triple point at 15.2 kbar and 686 K and then increases steeply with pressure. Clark and Rapoport [61] report the pressure dependence of KNO_2 (III–II) transition by DTA in a piston-cylinder device [62–65]. They used a 97.5 percent pure sample after two recrystallizations. The III–II transition was found to be from a completely ordered (NaCl like) phase to a partially disordered phase, whereas the II–I transition is from a partially disordered phase to a completely disordered NaCl phase [61]. Larionov and Livshits [66] have studied the polymorphic transformation (III–IV) at 15 kbar and 77–488 K and described the phase diagrams showing the relative disposition of the various phases.

Rubidium Nitrite, $RbNO_2$.

$RbNO_2$ is reported to undergo an endothermic phase transformation at ~ 348 K with $\Delta H_{tr} = 500 \pm 50$ cal mol^{-1} [1]. The DTA and electrical conductivity studies of Natarajan and Hovi [70] indicate an anomaly in the temperature range 340–390 K due to the phase transformation. Richter and Pistorius [69] have investigated the crystal structure and the pressure transformations of $RbNO_2$. According to them, $RbNO_2$ (phase I) at ambient conditions is cubic (space group $O_h^5 - Fm3m$, with $a = 6.934$ Å). It transforms at ~ 261 K to monoclinic $RbNO_2$ (phase II) with $a = 8.904$ Å, $b = 4.828$ Å, $c = 8.185$ Å, $\beta = 115.7°$ (determined at 271 K). $RbNO_2$ (II) appears to be ordered, whereas $RbNO_2$ (I) has a configuration entropy of Rln 32. The II/I transition line terminates at 0.3 kbar with appearance of $RbNO_2$ (phase III), a phase 17.3 percent denser than $RbNO_2$ (I). The II/III transition pressure increases with decreasing temperature to a triple point at 1.2 kbar, 208 K where a further dense phase IV appears. The II/IV transition pressure rises slightly with decreasing pressure. The melting curve of phase I passes through a maximum at 2.2 kbar, 663 K and is terminated at the III/I/liquid triple point at 5.2 kbar, 655 K. The melting curve of phase III rises with pressure.

Cesium Nitrite, $CsNO_2$, cubic, $O_h^1 - Pm3m$, $a = 4.34 \pm 0.02$ Å at ambient conditions [2].

Cesium nitrite seems to undergo an endothermic transformation at 393 ± 10 K with $\Delta H_{tr} = 1100 \pm 100$ cal mol^{-1} [1]. Protsenko and Kolomin [71] reported two phase transformations in $CsNO_2$ at 175 K and 353 K, respectively. The DTA and electrical conductivity studies by Natarajan and Hovi [70] indicate a thermal anomaly in 350–380 K temperature range, which they attribute to a phase transition. Richter and Pistorius [69] have reported $CsNO_2$ (phase I) to undergo a transformation at 179 K to a rhombohedral $CsNO_2$ (phase II, space group: $D_{3d}^5 - R\bar{3}m$ with $a = 4.307$ Å, $\alpha = 87°22'$). The II/I transition line is found to rise with pressure with an initial slope of 4.9 K/kbar.

Measurement technique	Observations	Remarks	References
X-ray diffraction.....	A new anomaly in dielectric constant is reported at 230 K. The cubic phase also appears just above 313 K. ΔV is very small during the 313 K transformation. The a-axis decreases while c increases at this point.	The absence of any superlattice reflections indicates some kind of disordered arrangement of the NO_2 groups. Ferroelectricity or antiferroelectricity is possible only below the room temperature.	[53, 54].
	After a thermal cycle traversing the transformation temperature to the high temp. form I, a single crystal of KNO_2 in phase II is converted into a hybrid crystal composed of domains of structure II in specific orientations. Detailed interpretation of some oscillation photographs of such a hybrid crystal in terms of composite reciprocal lattice demonstrates that the domain orientations are related by the point group symmetry m3.	It is concluded that form I must have a cubic structure. Consideration of the atomic displacements involved in the II $\rightleftharpoons$ I transformation show these to be consistent with a NaCl structure for form I; and also the lower cubic symmetry controlling domain orientations arises because of the physical requirement for the domains to coexist within the envelope of a 'single' crystal.	[68]
Differential thermal analysis...	KNO_2 undergoes a transition around 313 K... $\Delta H_{tr} \sim 120 \pm 30$ cal mol^{-1} ($\Delta T \sim 6$ K).	The observation was supported by studies of the temperature dependent infrared spectrum and a dielectric constant exhibiting around 313 K. Electrical conductivity also shows a slight break at 313 K. Protsenko et al. (3) report the phase transformation at 320 K.	[57, 69].
Differential Scanning Calorimetry.	$\Delta H_{tr} = 199 \pm 2$ cal mol^{-1}.....	.....	[38].
Spectroscopic, dielectric constant, and electrical conductivity measurements.	$T_c \sim 313$ K..... $P_s = 2.8$ μC cm^{-2}, $E_c - 160$V cm^{-1} at 298 K	Anomalies seen in $\epsilon(T)$ and $\sigma(T)$ plots.....	[3, 57, 69].
Dielectric constant and electrical conductivity.	Two clear transitions at ~ 260 K and 313 K are shown by anomalies in $\epsilon(T)$ and $\sigma(T)$ plots. The room temperature phase is rhombohedral with $R\bar{3}c$ symmetry.	The magnitude of dielectric anomaly does not suggest a ferroelectric-paraelectric transition in KNO_2 at 313 K.	[55].
	A new transition from orthorhombic (D_{2h}^{16} - aragonite type at 298 K) to a trigonal (close to D_{3d}^{6}-calcite type) structure is indicated by dielectric constant anomaly and loss studies. $T_t \sim 402$ K.	The transformation was not reversible and showed hysteresis.	[58].

References

[1] Natarajan, M., and Rao, C.N.R., unpublished results from this laboratory.

[2] Ferrari, A., Cavalca, L., and Tani, M. E., Gazz. Chim. Itali. **87**, 310 (1957).

[3] Protsenko, P. I., Bordyushkova, E. A., and Venerouskaya, L. N., Ukr. Khim. Zh. **31**, 1200 (1965).

[3a] Jona, F., and Shirane, G., Ferroelectric Crystals, Pergamon Press (1962), p. 361.

[4] Zheludev, I. S., and Sonin, A. S., Izv. Acad. Nauk SSSR, Ser. Fiz. **22**, 1441 (1958).

[5] Sawada, S., Nomura, S., Fujii, S., and Yoshita, I., Phys. Rev. Lett. **1**, 320 (1958).

[6] Sawada, S., Nomura, S., and Asao, Y., J. Phys. Soc. Japan **16**, 2207 (1961).

[7] Sonin, A. S., Zheludev, I. S., and Dobrzhanskii, G. F., Izv. Nauk SSSR, Ser. Fiz. **24**, 1209 (1960).

[8] Sonin, A. S., and Zheludev, I. S., Kristallografiya **8**, 57 (1963).

[9] Nomura, S., J. Phys. Soc. Japan **16**, 2440 (1961).

[10] Takagi, Y., and Gesi, K., J. Phys. Soc. Japan **19**, 142 (1964); **22**, 979 (1967).

[10a] Hamano, K., J. Phys. Soc. Japan **19**, 945 (1964).

[11] Nomura, S., Asao, Y., and Sawada, S., J. Phys. Soc. Japan **16,** 917 (1961).
[12] Tanisaki, S., J. Phys. Soc. Japan **16,** 579 (1961).
[13] Suzuki, S., and Takagi, M., J. Phys. Soc. Japan **21,** 554 (1966).
[14] Nomura, S., J. Phys. Soc. Japan **16,** 1352 (1961).
[15] Hoshino, S., J. Phys. Soc. Japan **19,** 140 (1964).
[16] Sakiyama, M., Kimoto, A., and Seki, S., J. Phys. Soc. Japan **20,** 2180 (1965).
[17] Hoshino, S. and Shibuya, I., J. Phys. Soc. Japan **16,** 1254 (1961).
[18] Naruyama, N. and Sawada, S., J. Phys. Soc. Japan, **20,** 811 (1965).
[19] Yoshida, I. and Sawada, S., J. Phys. Soc. Japan, **16,** 2467 (1961).
[20] Asao, Y., Yoshida, I., Ando, R., and Sawada, S., J. Phys. Soc. Japan **17,** 442 (1962).
[21] Betsayaku, H., J. Phys. Soc. Japan **21,** 187 (1966).
[22] Shibuya, I., J. Phys. Soc. Japan **16,** 490 (1961).
[23] Tanisaki, S., J. Phys. Soc. Japan **18,** 1181 (1963).
[24] Sato, Y., Gesi, K., and Takagi, Y., J. Phys. Soc. Japan **16,** 2172 (1961).
[25] Greenberg, J. and Hallgren, L. J., J. Chem. Phys. **33,** 900 (1960).
[26] Cleaver, B., Rhodes, E., and Ubbelohde, A. R., Proc. Roy. Soc. **A276,** 453 (1963).
[27] Chisler, E. V., Sov. Phys. (Solid State) **7,** 1825 (1966).
[28] Yamada, Y., Shibuya, I., and Hoshino, S., J. Phys. Soc. Japan **18,** 1594 (1963).
[29] Sawada, S., Yanagi, T., and Tokugawa, Y., J. Phys. Soc. Japan **20,** 834 (1965).
[29a] Flugge, S. and Meyenn, K. V., Z. Phys. **253,** 369 (1972).
[29b] Yamada, Y. and Yamada, T., J. Phys. Soc. Japan **21,** 2167 (1966).
[30] Mendiola, J., Canut, M. L., and Almoros, J. L., Acta Cryst. **16,** A190 (1963).
[31] Gesi, K., J. Phys. Soc. Japan **26,** 953 (1969).
[32] Bridgman, P. W., Proc. Amer. Acad. Arts Sci. **72,** 45 (1937).
[33] Lippincott, E. R., Weir, C. E., van Valkenberg, A., and Bunting, E. N., Spectrochim. Acta **16,** 58 (1960).
[34] Rapoport, E., J. Chem. Phys. **45,** 2721 (1966).
[35] Hoshino, S. and Motegi, H., Jap. J. Appl. Phys. **6,** 708 (1967).
[36] Mendiola, J., Electronica Fiz. Aplic. **10,** 5 (1967).
[37] Jaffray, J., J. recherches centr. natl. recherche sci. (Paris) 153 (1947).
[38] Adams, M. J. and House (Jr.), J. E., Trans. Ill. State Acad. Sci. **63,** 83 (1970).
[39] Gesi, K., Japan J. Appl. Phys. **4,** 817 (1965).
[40] Jaffray, J., Compt. Rend. **230,** 525 (1950).
[41] Myasnikova, T. P. and Evseeva, R. Ya., Krist. Fazorye Prevrashch, 41, (1971), Ed. by N. N. Sirota, Nauka i tekhnika Minsk., Beloruss (USSR).
[42] Gorelik, V. S., Zheludev, I. S., and Sushchinskii, M. M., Sov. Phys. cryst. **11,** 527 (1967).
[43] Chisler, E. V. and Shur, M. S., physica status solidi, **17,** 173 (1966).
[44] Chisler, E. V., Fiz. Tverd. Tela **7,** 2258 (1965).
[45] Chisler, E. V. and Shur, M. S., physica status solidi, **17,** 163 (1966).
[45a] Asawa, C. K. and Barnoski, M. K., Phys. Rev. (B) **2,** 205 (1970).
[46] Kaya, M. I. and Gonzalo, J. A., J. Phys. Soc. Japan Suppl. **28,** 284 (1969): published 1970.
[47] Rigamonti, A., Phys. Rev. Lett. **19,** 436 (1967).
[48] Oja, T., Marino, R. A. and Bray, P. J., Phys. Letters **26A,** 11 (1967).
[49] Kadaba, P. K., O'Reilly, D. E., and Blinc, R., physica status solidi **42,** 855 (1970).
[50] Gesi, K., J. Phys. Soc. Japan **20,** 1764 (1965).
[51] Gesi, K., Ozawa, K., and Takagi, Y., J. Phys. Soc. Japan **20,** 1773 (1965).
[52] Ziegler, G. E., Z. Krist, (A) **94,** 491 (1936).
[52a] Chang, S. C., Dissert. Abstracts **24,** 1668 (1963).
[53] Solbakk, J. K., and Strømme, K. O., Acta Chem. Scand. **23,** 300 (1969).
[54] Tanisaki, S. and Ishimatsu, T., J. Phys. Soc. Japan **20,** 1277 (1965).
[55] Mansingh, A. and Smith, A. M., J. Phys. D (Appl. Phys.) **4,** 560 (1971).
[56] Ray, J. D. and Ogg, R. A., J. Phys. Chem. **60** 1599 (1956).
[57] Rao, K. J. and Rao, C. N. R., Brit. J. Appl. Phys. **17,** 1653 (1966).
[58] Doucet, Y., Morabin, A., Tete, A., and Rostini, P., Compt. Rend. **261,** 3060 (1965).
[59] Bridgman, P. W., Proc. Amer. Acad. Arts Sci. **51,** 55 (1915).
[60] Hazlewood, F. J., Rhodes, E., and Ubbelohde, A. R., Trans. Faraday Soc. **59,** 2612 (1963).
[61] Clark, J. B. and Rapoport, E., J. Chem. Phys., **49,** 2453 (1968).
[62] Boyd, F. R. and England, J. L., J. Geophys. Res. **65,** 741 (1960).
[63] Kennedy, G. C. and Newton, R. C. in "Solids Under Pressure" Ed. W. Paul and D. M. Warschauer, McGraw Hill, New York (1963).
[64] Jayaraman, A., Klement, W. (Jr.), Newton, R. C., and Kennedy, G. C., J. Phys. Chem. Solids **24,** 7 (1963).
[65] Klement, W. (Jr.), Cohen, L. H., and Kennedy, G. C., J. Phys. Chem. Solids **27,** 171 (1966).
[66] Larionov, L. V. and Livshits, L. D., Izv. Akad. Nauk SSSR, Fiz. Zemli. **11,** 21 (1970).
[67] Parry, G. S. and Schuyff, Acta Cryst. **21,** 303 (1966).
[68] Sakai, K., J. Chem. Soc. Japan **75,** 182 (1954).
[69] Richter, P. W. and Pistorius, C. W. F. T., J. Solid State Chem. **5,** 276 (1972).
[70] Natarajan, M. and Hovi, V., Ann. Acad. Sci. Fenn. Ser. A. VI (400) 3 (1972).
[71] Protsenko, P. I. and Kolomin, L. G., Izv. Vuz. Fiz. (USSR) **7,** 105 (1971).

1.2. Alkaline Earth Metal Nitrites

(No crystallographic data seem to be available)

Polymorphic transformations in the nitrites of calcium, strontium, and barium have been reported from the anomalies in differential thermal analysis curves [1, 2] and electrical conductivity measurements [3]. Detailed studies, however, have not been carried out. The transformation temperatures for these nitrites are given below:

Nitrite	T_t, K
Calcium	539, 633
Strontium	458, 547
Barium	476, 503

References

[1] Protsenko, P. I. and Venerovskaya, L. N., Izd. Rostov. Gos. Univ. Rostov-on-Don 1960.

[2] Protsenko, P. I. and Brykova, N. A. Russ. J. Inorg. Chem. **8,** 1130 (1963).

[3] Kolomen, L. G. and Protsenko, P. I., Ukr. Khim. Zh. **36,** 1228 (1970).

1.3. Thallium Nitrite, $TlNO_2$

(No crystallographic data seem to be available)

Differential thermal analysis studies by Protsenko and Brykova [1] show a polymorphic transformation in $TlNO_2$ at 442 K. Earlier, Cuttica [2] reported the transformation temperature to be 404 K. Detailed studies, however, have not been made.

References

[1] Protsenko, P. I. and Brykova, N. A., Russ. J. Inorg. Chem. **8,** 1130 (1963).

[2] Cuttica, V., Alti. Acad. Lincei, Rend. Classe Sci. fis. mat. nat. **29,** 289 (1920).

2. Nitrates

Nitrates of many of the elements undergo phase transformations. Among these, alkali-metal nitrates and ammonium nitrate have been investigated extensively. Thermal as well as pressure transformations of nitrates have been studied by observing changes in crystallographic, thermodynamic, electrical, dielectric, magnetic and optical properties. We shall review these phase transitions of nitrates following the position of the element in the periodic table.

2.1. Nitric Acid, HNO_3

A single crystal of HNO_3 in equilibrium with its own liquid grown at a pressure of about 4 kbar has been found to exhibit a transition at room temperature and 8 kbar [1].

References

[1] van Valkenburg, A., Appl. Optics **9,** 1 (1970).

2.2. Alkali Metal Nitrates

As mentioned earlier, phase transformations of alkali metal nitrates have been studied in great detail and the subject has been reviewed by a few authors [1–3]. The orthorhombic-trigonal transformations in $NaNO_3$ and KNO_3, and the hexagonal-cubic transformations in $RbNO_3$ and $CsNO_3$ are well characterized. In this section, we shall examine the data on each of the alkali metal nitrates and provide the information in a tabular manner.

Lithium Nitrate, $LiNO_3$, rhombohedral (calcite type), $D_{3d}^6 - R\bar{3}c$, $Z = 6$ (for hexagonal cell) and 2 (for rhombohedral cell), $a = 4.692$ Å, $c = 15.22$ Å at 298 K.

The crystal structure of $LiNO_3$ was reported to be calcite type by Zachariasen [4]. The unit cell dimensions were later confirmed by Swanson et al. [5] at the National Bureau of Standards. There is no evidence for changes in the thermodynamic properties like specific heat and specific volume of $LiNO_3$ between room temperature and the melting point [6]. A study of the temperature variation of the electronic spectrum of $LiNO_3$ by Rhodes and Ubbelohde [7] shows that there is discontinuity in the absorption coefficient indicating a transformation. McLaren [1] concludes that if this is any indication of a transformation in $LiNO_3$, it could only be due to orientational disorder as in $NaNO_3$ (above ~ 458 K) or in NH_4NO_3 (in phase II). Fermor and Kjekshus [8] have measured the electrical resistivity and dielectric constant of $LiNO_3$ from 203 K to the melting point and report a transformation at 263 K, besides another anomaly at 503 K. Morabin et al. [9] have found the dielectric constant to increase linearly with temperature up to 483 K then followed by a faster rate of increase.

Sodium Nitrate, $NaNO_3$, rhombohedral, $D_{3d}^6 - R\bar{3}c$, $Z = 6$ (for hexagonal cell and 2 (for rhombohedral cell), $a = 5.0696$ Å, $c = 16.829$ Å at 298 K.

The structure of $NaNO_3$ was determined by Wyckoff [10] and the unit cell dimensions for the rhombohedral (calcite type) cell are $a = 6.3247$ Å and $\alpha = 47°16'$ at 296 K. Sodium nitrate has been found to undergo a phase transition from phase II, ordered rhombohedral phase (calcite type), to I, a disordered rhombohedral phase, around 548.5 K (I). Kracek et al. [10a] observed marked changes in the intensities of the x-ray reflections from some of the planes on heating $NaNO_3$ above ~488 K. They attributed this to the rotation of the NO_3^- ions about the trigonal axis. The investigations of Ketelaar and Strijk [11] also show that the transition is caused by internal rotation of the NO_3 groups in the crystal.

The most probable mode of rotation is that about an axis through the N-atom and perpendicular to the plane of the NO_3 group. Recently, Terauchi and Yamada [11a] have studied by x-ray scattering the phase transition of sodium nitrate crystal associated with the ordering of the orientation of NO_3^- ions. They have analysed the results on a microscopic basis and have concluded that the pair interactions between NO_3^- ions play an important role during the phase transition.

Anomaly in thermal expansion, DTA and heat capacity measurements were employed to study the transformation in $NaNO_3$ [12]. Around 548 K, dc electrical conductivity also shows a change in the slope [13]. Protsenko et al. [14] found $NaNO_3$ to be piezoelectric in the direction of the *b*-axis with a Curie point at 537 K. The dielectric constant had a sharp maximum in the vicinity of 437 K where the value is more than 100 times higher than that at room temperature. Dilatometric measurements showed the coefficient of linear expansion to be 10^{-4} per degree. Rhodes and Ubbelohde [7] noticed that the high energy absorption peak in the electronic spectrum of $NaNO_3$ shifted to lower wavelengths above ~ 548 K. Raman spectrum due to the internal vibrations of NO_3^- ions was studied by Chisler [15] to investigate the transition in $NaNO_3$. Earlier spectroscopic studies have shown that NO_3^- does not freely rotate above the transition temperature.

High Pressure Transformations: Polymorphic transformations at high pressure in alkali metal nitrates were investigated by Bridgman [16] up to 100 kbar. Jamieson and Lawson [17] made some preliminary but unsuccessful attempts to determine the crystal structure of the high pressure form of $NaNO_3$. Rapoport [18] showed that the pressure dependence of the transition in $NaNO_3$ could be described by the equation, $t = 275 + 6.076p - 0.038475p^2$, where t is temperature in degree centigrade and p is pressure in kbar.

$NaNO_3$

Measurement technique	Observations	Remarks	References
X-ray diffraction.....	A gradual transition (II⇌I) occurs by the formation of nuclei in the crystal matrix and their subsequent growth. Lattice constants for the two forms both of which have rhombohedral unit cell are: II $a = 6.32$ Å, $\alpha = 47°14'$ at 298 K I $a = 6.56$ Å, $\alpha = 45°35'$ at 553 K.	The transition depends upon the number of nucleating centers. At high temperatures, the nitrate groups seem to be statistically distributed between two twofold distorted, non-equivalent sets of position in rhomhedral unit cell.	[10a, 19–21].
Diffuse x-ray Scattering.....	.....	The observed ellipsoidal distribution of critical diffuse scattering in the reciprocal space has been explained by taking the pair interactions up to second nearest neighbours. The temperature-dependence of critical scattering gives a reasonable agreement with theoretical values in random phase approximation in the temperature range of $T > T_c + 4.5$ K. Both the temperature-dependence of long range order parameter and of anomalous lattice expansion can be satisfactorily explained by taking the strain dependence of pair interaction energy into account.	[11a].

Measurement technique	Observations	Remarks	References
	$T_t \sim 548$ K.....	Values of elasticity constants were deduced from intensity data and compared with elastic constants obtained by ultrasonic measurements. The diffuse maxima are believed to be a result of group-disorder. The maxima show strong angular dependence which is incompatible with the rotational model. The data fit a twofold disorder model for the nitrate groups provided that the positions have an aragonite type coordination with the surrounding Na atoms, rather than the calcite coordination found in the ordered structure.	[22, 23].
High pressure X-ray up to ~ 85 kbar.	Anomalous line intensity changes near 45 kbar are shown to be due to a transition from $R\bar{3}c$ to R3c space group without any change in volume.	The data suggest a higher order transition in which the nitrate groups in alternate layers along the trigonal axis rotate in opposite directions under pressure, and the nitrogen position is no longer planar with oxygen atoms. The atomic configuration suggests a ferroelectric phase and dielectric measurements indicate an anomaly at the transition point.	[24].
DTA and calorimetric measurements).	The specific heat curve shows a break beginning around 443 K and reaching a peak around T_t. $T_t = 549$ K. $\Delta H_{tr} = 1030 \pm 90$ cal mol^{-1}.	The behaviour of $NaNO_3$ has been discussed in terms of free rotation of nitrate ions. The transition is due to the transfer of NO_3^- from an ordered state to a disordered state.	[6, 25–29a].
Thermal conductivity, specific heat, thermal diffusivity, elasticity.	The abrupt change in thermal diffusivity is influenced by the abrupt change in the elastic constant S_{33}.	It is possible that above T_t the NO_3 groups may be rotated by 180° about the trigonal axis by means of lattice vibration.	[12, 27, 30].
	An impurity like calcium causes a decrease in the values of thermal characteristics of $NaNO_3$ near T_t. The decrease is proportional to the increase in calcium-concentration.	Thermal conductivity changes have been explained by the presence of an order-disorder scattering mechanism.	[30a].
Thermal expansion.....	A gradual transition ending to a peak value of coefficient of expansion at T_t followed by a rapid decrease to a normal value.	The transition occurring between 423 and 551 K is more marked along the c-axis than along the a-axis. The coefficients of thermal expansion increase monotonically with temperature up to the melting point.	[12, 27, 31–32a].
Differential thermal analysis (up to 40 kbar).	The effect of pressure on the gradual transition in $NaNO_3$ can be expressed by the equation. $T = 275 + 6.076p - 0.038475p^2$. T = temp (K), p = pressure (kbar).	.....	[18].
Permittivity measurements at 100 kHz.	Anisotropy is observed and unusual increase is seen in the (111) direction at 453 K and in the a-direction at 493 K. At this temperature, orientational polarization begins. At 548 K, the fixed position of NO_3^- ions does not exist and permittivity again decreases.	Thermal properties like thermal conductivity and thermal diffusivity behave in a similar manner.	[33].

$NaNO_3$—Continued

Measurement technique	Observations	Remarks	References
Dielectric constant and resistivity measurements (from room temperature to melting point).	At transition temperature maxima is observed in ϵ-T curve.	.....	[9, 24, 34].
Electrical conductivity measurements.	Conductivity-temperature curves show discontinuities or changes in slope near the transformation temperature.	.....	[13].
Infrared absorption spectra at different temperatures.	Assignments of the bands in the region, 3000–5000 cm^{-1} are made as librational combinations with vibrational bands. These bands persist in the temperature range between the IInd order transition and melting point, and disappear in the spectrum of the melt.	The thermal behaviour observed completely eliminates the hypothesis of free rotation of NO_3^- ions above the λ-point. The crystal structure above 548 K is disordered.	[35].
Raman Scattering.....	The intensity of the $NaNO_3$, 1385 cm^{-1} (ν_3) band in the range of 483–553 K increased rapidly ($T_t = 549$ K).	The strong asymmetric broadening of the line is attributed to the superposition of bands due to scattering by bound and quasi-free anions.	[15].
Ultrasonic and IR studies.....	$T_t \sim 549.7$ K.....	The results are interpreted on the basis that the 'frozen' elastic constant varies smoothly and monotonically with temperature throughout the transition region.	[36, 37].
		The intensity of the totally symmetric vibration ν_1, forbidden in the ordered but allowed, and weakly present, in the disordered phase, shows no sharp change in passing through the transition. This is consistent with the notion that short range order changes slowly with temperature in the transition region.	
	Strong frequency dependent ultrasonic attenuation is observed at temperatures immediately below and above the λ-point.	.....	
Garland relations applied to the λ-change in $NaNO_3$.	The transition is essentially one dimensional; most anomalies in properties do show up only in the c-direction.	.....	[38].

Potassium Nitrate, KNO_3, orthorhombic, D_{2h}^{16}-Pmcn, $Z = 4$, $a = 5.414$ Å, $b = 9.164$ Å, $c = 6.431$ Å at 299 K.

Potassium nitrate, form II (aragonite type), is the stable phase at 299 K and atmospheric pressure, and changes to form I (calcite type) at 403 K. On cooling, KNO_3 transforms from phase I to a new phase III at 397 K and from phase III to phase II at 383 K. The transformation in KNO_3 can be shown as follows [39].

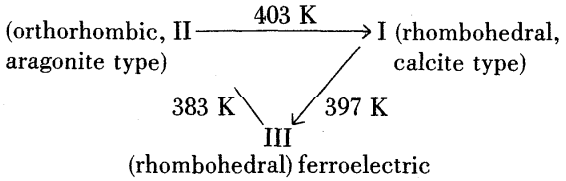

Fischmeister [39a] gave the unit cell dimensions for KNO_3 form I at 425 K as $a = 5.42$ Å and $c = 19.41$ Å which are in good agreement with the parameters reported by Tahvonen [39b]. This hexagonal cell contains 12 molecules. On heating, the unit cell of form I expands anisotropically, the marked expansion being along the c-axis (normal to the plane of anions). The expansion along the a-axis is slightly negative. This suggests that the linear vibration of NO_3^- is a more plausible form of disorder than the rotation in the plane about the N-atom. Form III has been reported to be ferroelectric [40] and is rhombohedral with $a = 5.43$ Å, $c = 9.112$ Å and space group C_{3v}^5-R3m at 388 K. Leonhardt and Borchert [41] as well as Kennedy et al. [42] have

studied the phase changes in single crystals of KNO_3 by x-rays.

Kracek [43] studied both moist and dry polycrystalline KNO_3 by DTA and observed an endothermic transition in the moist sample beginning around 403 K. On cooling, the sample gave an exothermic DTA peak beginning at 399 K. The forms above and below 400 K are I and II, respectively. The behaviour of the dry sample, however, was different, at least while cooling, where two exothermic peaks at 397 K and 382 K were noticed. The form stable in this temperature range is III. Oja [28] reports the II → I transformation at ~ 402.5 K from calorimetric studies.

Conductance studies on compressed polycrystalline pellets of KNO_3 were made by McLaren [1] who found the II → I transformation to occur at 399 K. The transitions were indicated by anomalous change in conductivity with increasing temperature [44]. Meinnel and Clinet [45] in their dielectric constant measurements found a sharp increase at ~ 400 K while heating and two distinct anomalies at ~ 380 K and ~ 368 K, while cooling.

Sawada et al. [40] showed that KNO_3–III is ferroelectric. The nature of ferroelectricity has been examined by Chen and Chernow [46], who measured the unit cell parameters of KNO_3 single crystals in the temperature region of the ferroelectric transition. The changes in the cell parameters as the crystal undergoes paraelectric to ferroelectric transition (I → III) have been interpreted as being due to the electrostriction effect.

Ferroelectricity in KNO_3 is due to the ordering of permanent dipoles. The permanent dipole in the paraelectric phase is believed to be due to the displacement of the nitrate ion from the center of the unit cell. The amplitude of this oscillation is 0.4 Å along the c-axis. If we consider, instead, that the structure is a disordered array of nitrate ions displaced from the center of the unit cell, the dipole moment per unit cell would be $\sim 9.8\ \mu c\ cm^{-2}$. This is very close to the value of spontaneous polarization in KNO_3. A double potential along the c-axis is considered to be a good model for explaining the NO_3^- ion displacement. A statistical theory based on this model and on the assumption of a lattice dependent internal field explains the origin of the electrostriction effect and observed anomalies at the ferroelectric transition. The statistical theory is related to Devonshire's thermodynamic theory of ferroelectric transition and good agreement is obtained between the theoretically predicted and experimentally determined coefficients of Devonshire's free energy. Balkanski and Teng [47] reported a normal vibration analysis of all the three phases of KNO_3 and found a close correspondence between normal modes of different phases. They also report a complete KNO_3 phase transition cycle in Raman Scattering. On heating, all the ionic and rotational modes in phase II were found to vanish abruptly at 403 K suggesting that the transition II→I is of a rather sudden nature. A notable and continuous broadening of the rotational mode at 83 cm^{-1} was also observed near T_t. Between 383 and 373 K, on cooling, the spectra suggest that the limits between phase III and II may be less precise and that the III→II phase transition probably occurs more gradually than the other phase transition.

High Pressure Transformations: The phase diagram of KNO_3 reported by Bridgman [48] in the pressure range 0–12 kbar up to 473 K, revealed two rhombohedral (I and III) and two orthorhombic (II and IV) phases. The polymorphs III and IV are the high pressure forms. KNO_3–III, however, could be attained metastably at atmospheric pressure and its crystal structure was reported by Barth [49] as rhombohedral with $Z = 1$ with the NO_3^- ion displaced some six percent above the cell center. Davis and Adams [50] studied the kinetics of the phase transformations I ⇌ II and II ⇌ III at high pressures in detail. Rapoport and Kennedy [51] have examined the high pressure transformations in KNO_3 up to 40 kbar and 873 K employing DTA. They found as many as seven polymorphs, phases V, VI, and VII being entirely new. The phase diagram of KNO_3 above 15 kbar was found to closely resemble that of $RbNO_3$, $CsNO_3$ or $TlNO_3$ and it is suggested that KNO_3 VII encountered at 30 kbar is structurally similar to the phases found by Bridgman [52] in $RbNO_3$ at 24 kbar and in $CsNO_3$ at 27 kbar.

<table>
<tr><th>Measurement technique</th><th>Observations</th><th>Remarks</th><th>References</th></tr>
<tr><td>X-ray diffraction.....</td><td>T_t = 401 K for orthorhombic to rhombohedral transformation. While cooling, the solid obtains a mosaic character at 396 K and at 386 K changes to a finely divided material.</td><td>The changes at 396 K and 386 K are due to the I–III and III–II transformations in KNO_3. Crystals of the high temperature phase grow rhythmically from the low temperature phase to form discrete and easily identifiable layers.</td><td>[41, 42, 53–55].</td></tr>
<tr><td></td><td>Single crystals preserve their nature with very slow heating rates. The (110) plane of the calcite-type crystal parallels the (010) plane of the original aragonite-type crystal. An incubation period averaging 4.1 minutes exists for the transformation. Structural transformations are completely reversible. The volume change at the phase boundary is 0.71 percent.</td><td>The c-axes of the two structures are not parallel but differ by 26° both lying in the plane common to the two structures. In moist crystals, the b-axis shows a marked persistence with respect to original b-axis. The a and c axes often undergo rotation about the original direction of the b-axis. The direction of none of the original axes persists in rigorously dried crystals.</td><td></td></tr>
<tr><td></td><td>A new transition at 213 K was found, showing marked hysteresis effects.</td><td>From the new phase, the material slowly transformed to the stable, normal II phase at 299 K.</td><td>[56].</td></tr>
<tr><td>High Pressure x-ray diffraction.</td><td>The structural information for the high pressure phases III and IV are as follows:
<table>
<tr><th>Phase</th><th>Pressure, kbar</th><th>Temp., K</th><th>Structural information</th></tr>
<tr><td>III</td><td>2.5</td><td>406</td><td>Hexagonal pseudo-cell, $Z = 6$, $a = 5.44_0$ Å, $c = 17.51_6$ Å</td></tr>
<tr><td colspan="4">($\Delta V \sim 0.036$ cm^{3}g^{-1} at 410 K and 0.5 kbar)...</td></tr>
<tr><td>IV</td><td>3.0</td><td>298</td><td>Orthorhombic $Z = 10$ space group $P_{mn}2_1$ (for K^+ ions) $a = 11.048$ Å, $b = 8.367$ Å $c = 7.402$ Å.</td></tr>
</table>
Several diffraction patterns of the transitions I–II and III–II revealed preferred orientation of grains in the resulting aragonite type phase. Cell parameters of KNO_3–I and KNO_3–III (both modified calcite structures) taken in their stability fields show a marked reduction in the c-axis length going from phase–I to phase–III with increasing pressure at constant temperature.</td><td>Rate studies on the transition KNO_3 II $\rightleftharpoons$ IV showed an overall approach to first order kinetics but in detail, reveal several growth stages.
The transitions are only partially manifested by an uneven change in the pressure. The change was found gradual, in many cases, over a temp. interval, and the pressure curve before and after rectilinear. In such cases the intersection of these two rectilinear portions give the transition point.</td><td>[48, 50, 57, 58].</td></tr>
<tr><td>Differential Thermal Analysis.</td><td>
<table>
<tr><th>Transition</th><th>ΔH_{tr}, cal mol^{-1} (approx.)</th><th>E_a, kcal mol^{-1}</th></tr>
<tr><td>II→I</td><td>1200</td><td>100</td></tr>
<tr><td>I⇄III</td><td>820</td><td>—</td></tr>
<tr><td>III⇄II</td><td>820</td><td>—</td></tr>
</table></td><td>The thermal hysteresis, (ΔT), is linearly related to the differences in volume of the transforming and the transformed phases.</td><td>[25, 59–60a].</td></tr>
</table>

Measurement technique	Observations	Remarks	References
Particle size effects in the II→I transition by DTA.	Particle size μ(micron) / T_t, K / ΔH_{tr}, cal mol^{-1}: 5.5, 413, 1450; 49.5, 413, 1200; 115.0, 406, 1000; 137.0, 403, 1050	T_t decreases with the particle size while ΔH_{tr} also shows a progressive decrease. These effects are related to non-attainment of thermodynamic equilibrium and surface energy factors. Effect of heating rates on T_t is also discussed.	[61].
Thermal analysis and dilatometry, up to 300 Mbar.	T_t for II→I change is affected by moisture. At 50 Mbar $\Delta V = 0.00484$ cm^{3}g^{-1} for the II→I transition; at 151 Mbar, $\Delta V = 0.0087$ cm^3 g^{-1} for II→III and at 251 Mbar $\Delta V = -0.0091$ cm^3 g^{-1} for III→I.	Conditions for metastability of KNO_3–III at atmospheric pressure are discussed.	[43].
High pressure DTA up to 873 K and 40 kbar.	The melting curve passes through a broad maxima at 6.4 kbar, possibly through a second maxima at 11 kbar and then rises steeply with increasing pressure above 15 kbar.	Three new polymorphs V, VI, and VII were found. The phase diagram of KNO_3 seems very similar to that of $RbNO_3$ or $CsNO_3$.	[51].
Kinetics of III→II transition.	The III→II transition may be described by two first order processes, and each of these can be expressed by a single rate constant.	The existence of ferroelectric behaviour in the phase III polymorph permits direct recording of the rate of transition of the phase III→phase II at temperatures far removed from the normal T_t at atmospheric pressure.	[63].
Dielectric constant.....	The real part of ϵ varies from 4.45 to 12.10 and the losses from several thousandths to 0.68 with increasing temperature. The transition is reversible and exhibits hysteresis.	In samples subjected to gamma rays, the P_s shows substantial decrease and E_c values show increase. No double hysteresis loop was observed. Results show phase III having two Curie points; the upper T_c increases while the lower T_c decreases with increasing pressure up to ~ 1.38 kbar (20,000 psi).	[35, 46, 64–68].
Electrical conductivity, dielectric constant and dielectric loss.	Anomaly is observed at ~ 403 K on heating and at ~ 397 and 381 K on cooling.	The occurrence of a relaxation type of dielectric dispersion in the microwave region together with the contraction of the ferroelectric axis at the transition, suggests that ferroelectricity in KNO_3 is an order-disorder phenomena.	[48, 69, 70].
Dielectric constant and spontaneous polarization.	The isothermal and isobaric I→III transition exhibited sharp dielec. peaks at all pressures, with ϵ_{max} increasing with pressure. KNO_3–I obeys a pressure Curie-Weiss law, with $\left(\frac{1}{\epsilon(p)}\right)_{T'} = \frac{p-p_0}{C^*}$ at $T' = 433$ K, $C^* = -276$ kbar and $p_0 = 4.68$ kbar. The KNO_3 II→III isobaric transition involves a small jump in ϵ (from 5 to 7.5 at $p = 1.7$ kbar) followed by a speedy increase up to the III→I boundary. Polarization loops were obtained in KNO_3–III with $P_s(p)$ reaching a maximum of 8μ coulomb/cm^2. Metastable KNO_3–		[71].

Measurement technique	Observations	Remarks	References
	III was observed at room temperature and room pressure after specimens had first been exposed to high pressures (1.7–4.0 kbar) while in region III. In KNO_3–I, $K' = dT_0/dp$ is approximately 25 k/kbar.		
Electrical conductivity.....	All the transitions are shown by conductivity temperature curves. The II→I, III→I and I→III phase transitions follow the kinetic equation $$\ln \alpha/(1-\alpha) = kT + c,$$ where α is the degree of conversion and t is the time.	The phase transitions of KNO_3 are volume reactions with a complete mutual dispersion of both phases; the course of the reaction is controlled by nucleation.	[72–74].
Infrared spectroscopy.....	The transitions of KNO_3 at 403,398, and and 388 K are associated with changes in the positions of bands at 720, 830, and 1055 cm^{-1} characteristic for the internal vibrations of NO_3. The temperature dependence is also given by the lattice vibrations along a, b, and c axes.	The analysis indicates that in the phase I the NO_3^- ions are randomly oriented.	[75–79].
Far infrared reflectivity spectra over the range 20–400 cm^{-1}.	The two infrared active lattice modes observed are described by parameters obtained from a classical oscillator analysis, which was confirmed by Kramers-Kronig analysis.	From the temperature dependence of the mode parameters and their contribution to their dielectric constant it was concluded that the paraelectric phase I is a disordered arrangement of electrical dipoles. Thus the paraelectric to ferroelectric transition is an order-disorder transition.	[80].
Electron paramagnetic resonance of Mn^{+2} in KNO_3. KNO_3.	The hyperfine coupling constant, half width, and line intensity show sudden changes at the T_t. The lines are much sharper in the high temperature phase of the crystal.	The observed changes are explained in terms of structural changes and NO_3^- ion rotation. Indications of the presence of a metastable γ-phase (ferroelectric phase) has also been found.	[81].
Polarising microscope with hot stage.	On heating, the transition boundary B_{II-I} starts from hot end of the crystal and moves on to the other end making the specimen somewhat polycrystalline. Further heating, brings about recrystallization. On cooling, the boundary B_{I-III} appears on the cooler end subsequently followed by B_{III-II} boundary.	The boundary B_{III-II} usually leaves many cracks after its passage. However, the speed of the boundary B_{I-III} is rather small as compared with that of the boundary B_{III-II}, and shortly after their appearance the boundary B_{III-II} often catches up with the boundary B_{I-III}. Thereafter, the united boundary B_{I-II} proceeds further to the hot end leaving no more cracks.	[82].
Ultraviolet spectroscopy.....	A gradual shift of absorption bands is found to accompany thermal expansion of the crystals and an abrupt change is seen at T_t, transformation showing hysteresis at 313 K has been detected.	The technique proves a sensitive means for the study of various thermodynamic effects in phase transformations.	[83].

KNO_3 – Continued

Measurement technique	Observations	Remarks	References
Raman Scattering.....	In the ferroelectric phase a significant intensity increase was noted for all the covalent modes. A broad band at ~120 cm^{-1} is observed in the ferroelectric phase, the half-width of this band depends upon temperature. Two new lines at 65 and 133 cm^{-1} are found in the room temperature phase.	Raman active modes in different crystal structures have been correlated. Strong asymmetric broadening of the line may be regarded as the result of superposition of bands due to scattering by bound and quasi-free anions. From theoretical considerations it is concluded that C_{3v}^3 is the most suitable space group to describe KNO_3–I, the high temperature phase.	[15, 84–86].
Raman Spectra study of ferroelectric transition under pressure up to 800 bar (from room temperature to 418 K).	The lattice dynamical behaviour of the direct high pressure II–III phase transition is quite similar to that under atmospheric condition.	The structures of II and III phases are very close to one another. Raman spectra of the ferroelectric phase reveals that at high pressure, KNO_3–III is more stable than at atmospheric pressure.	[87].
Neutron diffraction at high pressures.	The pressure phase IV of KNO_3 at ~15 kbar is noticed.	.....	[88].
Viscosity measurements.....	Show evidence for II→I transition.	.....	[89].
Change in grain size.....	Number of grains per unit area increased from 4 to 70 during transformation at 393 K.	.....	[90].

Rubidium Nitrate, $RbNO_3$, Trigonal, $C_{3v}^3 = P31m$, $Z = 9$, $a = 10.479$ Å, $c = 7.452$ Å, at 298 K.

It has been established by x-ray diffraction [91–95], DTA [25, 96], dilatometric [83, 91], calorimetric [97–99], electric conductivity [1, 100, 101] and optical [83] measurements that $RbNO_3$ undergoes the following phase transformations:

$$\text{IV} \xrightarrow{437\,\text{K}} \text{III} \xrightarrow{492\,\text{K}} \text{II} \xrightarrow{564\,\text{K}} \text{I}$$

(Trigonal) (Cubic) (Rhombohedral) (Cubic)
CsCl type NaCl type

Single crystal photographs at ~ 453 K suggest that $RbNO_3$–III is cubic with $a = 4.36$ Å containing only one molecule per unit cell. Korhonen [102] however, assigns a value of a twice as this from his studies of powder photographs, i.e., $a = 8.72$ Å with $Z = 8$. X-ray photographs of $RbNO_3$ single crystals heated through the IV → III transformation indicate that the trigonal triad [00.1] of IV is transformed to the cubic triad [111] of III with the trigonal [10.1] direction becoming the cube edge direction [100]. Thus, during the III → IV transition any one of the four equivalent cube diagonals can give rise to the trigonal c-axis. Hence, in the transformation cycle, IV → III → IV, the crystals may come back to form IV in any of four orientations [101]. All these possibilities were observed. Accordingly, Finback and Hassel [103] suggest that the NO_3^- ions are in free rotation in form III. Korhonen [102] suggests that the anion disorder is akin to the one in KNO_3 suggested by Fischmeister [39]. Form II is rhombohedral with $a = 4.8$ Å, $\alpha = 70°28'$ (around 520 K) having one molecule per unit cell. Form I is cubic with one molecule per unit cell; $a = 7.32$ Å at ~ 573 K.

The thermal transformations in $RbNO_3$ were studied by DTA by Plyushchev et al. [96, 104] and Rao and Rao [25]. The electrical conductance of compressed powder pellets of $RbNO_3$ has been reported by Brown and McLaren [101]. The IV–III transition is marked by an increase in conductance by two orders of magnitude. After cycling, the conductance changes by a factor of 30 at the III–II transition in both the directions. Cycling also produces a change by three orders of magnitude in the

IV–III transition in both the directions. These results were reproducible. The II–I transition is characterized by a change in the slope of the conductance curve.

Meinnel and Clinet [45] found an anomalous increase in dielectric constant (ϵ) at ~ 323 K. On cooling, the fall in ϵ was observed at ~ 313 K. Finback and Hassel [105] reported that $RbNO_3$–IV is pyroelectric. Dantsiger [34] concludes from dielectric and dilatometric studies that $RbNO_3$ has ferroelectric properties between the first and second phase transition points. Examination of single crystals of $RbNO_3$ by an optical microscope [1] shows that it crystallizes in the form of *c*-axis needles which are anisotropic and show parallel extinction. On heating, the IV→III change was noticed at ~430 K with the crystals becoming isotropic. It is interesting to note that while cooling (i.e. III→IV transition) the crystals retained their external shape as well as their single crystal character. Further heating results in the cracking of single crystals through the III→II transition at ~ 500 K, and the crystals also become anisotropic. Around 563 K, the crystals become isotropic without further distortion.

High Pressure Transformations: Bridgman [52, 106] reported new polymorphs in $RbNO_3$ in the pressure and temperature ranges 0–50 kbar and 194–473 K, respectively, by his piston displacement method. Later he extended his measurements up to 100 kbar [16]. In his earlier work, Bridgman found similarity in the phase diagrams of $RbNO_3$ and $CsNO_3$ [48]. Rapoport and Kennedy [51, 107] also showed that the phase diagram of $RbNO_3$ above 2 kbar is quite similar to that of KNO_3 above 15 kbar and of $CsNO_3$. The corresponding phases have been found to be isostructural.

$RbNO_3$

Measurement technique	Observations	Remarks	References
X-ray diffraction.....	Transition / T_t, K: IV→III 437; III→II 492; II→I 564	Structures IV, III, and II are related to one another while II and I are not related. Transitions between IV, III, and II appear to involve changes of positional randomization of Rb^+. No evidence was available for such randomization in II→I transition. $RbNO_3$–II is rhombohedral and not tetragonal as suggested earlier [97]. This is confirmed by data from x-ray and dilatometric studies. The polymorphism in $RbNO_3$ seems to be sensitive to a temperature dependent effective ionic radius of the anion. X-ray and optical studies on single crystals of $RbNO_3$ indicate incomplete randomization of the NO_3^- ion orientations.	[93, 95, 101–103, 108–110].
Differential thermal analysis and thermoanalytical measurements.	Transition / ΔH_{tr} cal mol^{-1} / E_a kcal mol^{-1} / ΔS_{tr} cal mol^{-1} deg^{-1} / ΔV %: IV–III 950 165 2.11 2.1; III–II 650 50 1.53 10.0; II–I 300 55 0.42 1.0	The thermal hysteresis is related to the differences in volume of the transforming and transformed phases.	[2, 25, 96, 104, 108, 111].
	The measurements under improved conditions revealed five endotherms for $RbNO_3$.	The first four endotherms at 440, 509, 563, and 575 K respectively are due to crystal transitions and the fifth one at 587 K is due to fusion.	[112].
Calorimetric measurements..	The transition energies have been reported...	No phase transition was observed below room temperature as reported earlier by Fermor and Kjekshus [70].	[97, 99, 113].

$RbNO_3$—Continued

Measurement technique	Observations	Remarks	References
Electric conductivity.....	Discontinuities in the plot of log σ versus $1/T$ are observed at all the transition points. IV–III transition at 431 K is marked by an increase in σ by a factor of 1000; the III→ II transition at 495 K is accompanied by a decrease in σ by a factor of 100; finally the II→ I transition at 559 K is indicated by a change in the slope. Cerisier and Guitard [114] find the results different from Brown and McLaren [101].	The conductivity behaviour is explained in terms of the crystal structure changes in $RbNO_3$.	[1, 74, 100–102, 114, [115].
Dielectric and dilatometric measurements.	At 434 and 471 K $RbNO_3$ undergoes considerable shrinkage and its dielectric constant increases considerably; at 471 K, Curie-Weiss law is followed with a Curie constant of 4.7×10^3. Dependence of ϵ and tan δ on field intensity (50Hz) of an alternating electric field at 370 and 428 K are given. As the point of phase transition is approached, the non-linearity increases.	It is hypothesized that $RbNO_3$ has ferroelectric properties below the point of the first phase transition and above the point of second phase transition. No transformation below room temperature was observed.	[37, 40]
	The hysteresis energy of the III⇌IV transition ($T_t\sim437$ K) is a few thousandth of the ΔH_{tr}. It varies with the purity of the sample. ($\Delta V\sim0.903$ cm^3 mol^{-1} at T_t.)	The transition in $RbNO_3$ is a symmetry controlled transformation. The transition is discontinuous and the expansion coefficient of the cubic form is normal and positive.	[94, 116].
Optical measurement.....	The temperature dependence of the ν_3 vibration frequency as well as that of lattice vibration along a, b, and c axes are studied.	.....	[78, 101, 117].
Ultraviolet spectroscopy	The ultraviolet absorption bands shifts are observed at T_t. ΔV have been reported for various transformations.	The shifts in absorption bands are abrupt in cases where a crystal structure change accompanies the transition. In the cases of known crystal structure, these shifts have been correlated to changes in interatomic distances between cations and anions.	[83].
Nuclear magnetic resonance spectra of ^{14}N nuclei	Nuclear electric quadrupole coupling constants, assymmetry parameters of the N-nuclei and the orientation of groups with respect to the crystallographic axis are determined.	.....	[118].

Cesium Nitrate, $CsNO_3$, hexagonal, C_{3v}^2—P31m, $Z=9$, $a=10.87$ Å, $c=7.76$ Å below 434 K [118a].

Cesium nitrate undergoes a phase transformation around 434 K from phase II (hexagonal) to phase I (cubic) [103, 105, 119]. The reverse transformation (I→II) takes place at a lower temperature (~422 K) showing considerable hysteresis. Phase I has been reported to be cubic with $a=4.499$ Å at ~400 K and $Z=1$ [103]. Ferroni et al. [119] have, however, suggested that the true unit cell should have eight such cubic units i.e. $Z=8$ with $a=8.98$ Å. This doubled cell parameter agrees well with the one given by Korhonen [120], who reports the space group for this phase to be Pa3. Finbak and Hassel [103] observed that the single crystals of $CsNO_3$ when heated above 473 K, were not destroyed.

Single crystal photographs of $CsNO_3$ taken at 298, 473, and again at 298 K show that the Cs^+ ion sub-lattice is very similar in both the structures. This indicates that the structure of $CsNO_3$ (I) is a slightly distorted version of the $CsNO_3$ (II) structure. According to Ferroni and others, the difference in structures of phases I and II is due to changes in the orientation of the NO_3^- ion, the Cs^+ ion position being practically the same. Cini and Cocchi [121], from magnetic measurements, have shown that the high temperature phase is a centrosymmetric one, and is cubic.

DTA anomalies are reported by Plyuschev et al. [96, 104], Rao and Rao [25] and others. Sato [124] found a specific heat anomaly in 418–434 K range. Electrical conductivity measurements on polycrystalline pellets were made by McLaren [1] who found a rise in conductivity at T_t and a decrease in conductivity at 427 K on cooling. The conductivity changes by a factor of 3 on heating as well as on cooling. Meinnel and Clinet [45] measured the dielectric constant of $CsNO_3$ and found an anomaly at 393 K both on heating and cooling. Finbak and Hassel [105] report from single crystal studies that $CsNO_3$–II is pyroelectric. Single crystals of $CsNO_3$ under a polarizing microscope showed no destruction of these crystals on cycling through the transition. There was, in general, no appreciable change in the orientation of form II after thermal cycling (i.e. II→I→II) [1, 104].

High Pressure Transformations: Bridgman [52, 106] reported new polymorphs in $CsNO_3$ in his high pressure investigations up to 50 kbar in 193–473 K range. He showed a similarity between the diagrams of $RbNO_3$ and $CsNO_3$ [48]. The phase diagrams of $CsNO_3$ were found to be quite similar to those of KNO_3, above 15 kbar, and $RbNO_3$, above 2 kbar by Rapoport and Kennedy [51, 107], who found the corresponding phases to be isostructural. Structural information on the high pressure polymorphs has not been reported in the literature.

$CsNO_3$

Measurement technique	Observations	Remarks	References
X-ray diffraction.....	Above 434 k (T_t) the structure due to Cs^+ ions is rhombohedral with $a=4.45$ Å and $\alpha=89°40'$. However, the NO_3^- ions within the various "Cs^+ only" rhombohedral cells are not equivalent. Consequently, the unit cell for $CsNO_3$ is larger containing nine of the smaller units and with $a=10.87$ Å and $c=7.76$ Å.	The form below 434 K, is cubic with $a=4.49$ Å with one $CsNO_3$ per unit cell [55]. However, Ferroni et al. [117] believe that the unit cell must include 8 of the smaller units with $a=8.98$ Å. Free rotation of NO_3^- ions is a questionable hypothesis since the diameter of a freely rotating spherical NO_3^- is larger than Cs-Cs distance along the ternary axis. The two structures differ only in NO_3^- ion orientation.	[103, 105, 119, 120].
Differential Thermal Analysis.	T_t, 434 K. $\Delta H_{tr} \sim 350$ cal mol $^{-1}$. $E_a \sim 75$ kcal mol^{-1}.	The thermal hysteresis is linearly related with the change in volume of the transforming and the transformed phases.	[25, 96, 104, 122].
Calorimetric measurements..	T_t is reported to be 424.5–425 K. No phase transformation below room temperature was observed (also see ref. 66). $\Delta H_{tr}=893\pm80$ cal mol^{-1}. The molecular specific heats of $CsNO_3$ up to the transition point were found to be represented by the following equation: $C_p=9.84+46.4\times10^{-3}T$ for $T=273-373$ K.	Free rotation of NO_3^- in $CsNO_3$ is reduced from the variation of molar heat with temperature.	[113, 123, 124].
Dilatometry.....	Transition at 434 K is first order. The expansion coefficient of the cubic form is normal and positive.	Hysteresis effects are sensitive to recrystallization and aging of the sample.	[94].
Electrical conductivity.....	The transformation is marked by a sharp change in conductivity.	.....	[1, 125].
Dielectric constant and resistivity (193–303 K).	Anomaly is observed at point of phase transformation.	.....	[70].

$CsNO_3$—Continued

Measurement technique	Observations	Remarks	References
Optical examination in polarized light, polarized infrared and laser induced Raman spectroscopy.	The spectra of single crystals of $CsNO_3$–II in the region of the internal vibrations of NO_3^- indicate that these ions are positioned at sites having C_1 symmetry and the unit cell symmetry of the trigonal space group is $C_3^1(C_3)$.	Raman spectra of the lattice vibrations are presented.	[105, 126, 127].
Ultraviolet spectra.....	Ultraviolet absorption band gradually shifts accompanying the transition at ~ 426 K.	The shifts in absorption maxima due to changes in temperature are interpreted in relation to changes in interionic distance.	[83].
Magnetic investigations.....	Single crystals of $CsNO_3$ when held in a magnetic field behave anomalously while being heated carefully. This effect known as polyelectricity disappears at 437 K. By a technique in which powder $CsNO_3$ is held in a sphere suspended in a uniform magnetic field, the anisotropic packing of the magnetically anisotropic cesium nitrate causes a torque which is constant up to 437 K at which point it is completely nullified.	The observations confirm the centrosymmetry and cubic classification of the high temperature phase.	[121].

References

[1] McLaren, A. C., Rev. Pure Appl. Chem., **12,** 54 (1962).
[1a] Rao, K. J., Ph.D. Thesis, Indian Institute of Technology, Kanpur (1967).
[2] Newns, D. M. and Staveley, L. A. K., Chem. Rev. **66,** 267 (1966).
[3] Jaffray, J., Ann. Phys. [12], **3,** 5 (1948).
[4] Zachariasen, W. H., Skrifter, Norske Videnskaps-Akad. Oelo I. Mat-Naturv. Kl 1928, No. 4 (1928), p. 27.
[5] Standard X-ray Diffraction Powder Patterns, N.B.S. Circular 539. Ed. Swansen, H. E. et al., vol. 7, p. 27 (1957).
[6] Gordon, S. and Campbell, C., Anal. Chem. **27,** 1102 (1955).
[7] Rhodes, E. and Ubbelohde, A. R., Proc. Roy. Soc. **A251,** 156 (1959).
[8] Fermor, J. H. and Kjekshus, A., Acta Chem. Scand. **23,** 1581 (1969).
[9] Morabin, A., Tete, A., Santini, R., and Habert, M., C.R. Acad. Sci. Sec. B, **269,** 489 (1969).
[10] Wyckoff, R. W. G., Phys. Rev. **16,** 149 (1920).
[10a] Kracek, F. C., Posnjak, E., and Hendricks, S. B., J. Am. Chem. Soc. **53,** 3339 (1931).
[11] Ketelaar, J. A. A. and Strijk, B., Rec. Trav. Chim. **64,** 174 (1945).
[11a] Terauchi, H. and Yamada, Y., J. Phys. Soc. Japan **33,** 446 (1972).
[12] Kracek, F. C., J. Am. Chem. Soc. **53,** 2609 (1931).
[13] Jaffray, J., Compt. Rend. **230,** 525 (1950).
[14] Protsenko, P. I., Khodakov, A. A., Mirskaya, E. Z., and Venerovskaya, L. N., Segn. Rost.-na-Donu Gos. Univ. Nauchr.-Illted, Fiz. Mat. Inst., Sb. Statei, 21 (1961).
[15] Chisler, E. V., Sov. Phys. (Solid State) **7,** 1283 (1965).
[16] Bridgman, P. W., Proc. Amer. Acad. Arts Sci. **76,** 1 (1945); Rev. Mod. Phys. **18,** 1 (1946).
[17] Jamieson, J. C. and Lawson, A. W., J. Appl. Phys. **33,** 776 (1962).
[18] Rapoport, E., J. Phys. Chem. Solids **27,** 1349 (1966).
[19] Asadov, Yu. G., Sov. Phys. (Crystallography) **12,** 537 (1967).
[20] Wilman, H., Proc. Phys. Soc. (London) **64A,** 329 (1951).
[21] Strømme, K. O., Acta Chem. Scand. **23,** 1616 (1969).
[22] Mendiola, J., Rev. Cienc. Apl. (Madrid) **20,** 487 (1966).
[23] Siegel, L. A., J. Chem. Phys. **17,** 1146 (1949).
[24] Barnett, J. D., Pack J., and Hall, H. T., Proc. Symp. Crystal Structure at High Pressure, Seattle, Wash., U.S.A., March (1969).
[25] Rao, K. J. and Rao, C. N. R., J. Mat. Sc. **1,** 238 (1966).
[26] Mustajoki, A., Ann. Acad. Sci. Fenn. Ser. A VI, No. 5, 17 (1957).
[27] Semenchenko, V. K., and Al-Khayat, B. Kh., Zh. Fiz. Khim. **42,** 2634 (1968).
[28] Oja, H. M., Chem. Zentr. II, 303 (1943).
[29] Reinsborough, V. C. and Wetmore, F. E. W., Aust. J. Chem. **20,** 1 (1967).
[29a] Schuermann, E. and Nedeljkovic, Lj., Ber. Bunsenges. Phys. Chem. **74,** 462 (1970).
[30] Kubicar, L., Fyz. Cas., Slov. Akad. Vied. **18,** 58 (1968).
[30a] Dikant, J., Czech. J. Phys. **B22,** 697 (1972).
[31] Austin, J. B. and Pierce, R. H. H. (Jr.), J. Amer. Chem. Soc. **55,** 661 (1933).
[31a] Kaya, M. I. and Gonzalo, J. A., J. Phys. Soc. Japan Suppl. **28,** 284 (1969).
[32] Kracek, F. C. and Posnjak, E., J. Amer. Chem. Soc., **53,** 1183 (1931).
[32a] Rao, K. V. K. and Murthy, K. S., J. Phys. Chem. Solids, **31,** 887 (1970).

[33] Kubicar, L. and Mariani, E., Fyz. Cas. **18,** 251 (1968).
[34] Dantsiger, A. Ya, Nauchn. Konf. Aspirantov **75,** (1962).
[35] Hexter, R. M., Spectrochim. Acta **10,** 289 (1958).
[36] Craft, W. L. (Jr.), Eckhardt, R., and Slutsky, L. J., J. Phys. Soc. Japan, Suppl. **26,** 184 (1968).
[37] Craft, W. L. and Slutsky, L. J., J. Chem. Phys. **49,** 638 (1968).
[38] Klement, W. (Jr.), J. Phys. Chem. **72,** 1294 (1968)
[39] Jona, F. and Shirane, G., Ferroelectric Crystals, Pergamon Press (1962), p. 360.
[39a] Fischmeister, H. F., J. Inorg. Nucl. Chem. **3,** 182 (1956).
[39b] Tahvonen, P. E., Ann. Acad. Sci. Fenn., Ser. AI, 44 (1947).
[40] Sawada, S., Nomura, S., and Fujii, S., J. Phys. Soc. Japan **13,** 1549 (1958).
[41] Leonhardt, J. and Borchert, W., Naturwiss. **24,** 412 (1936).
[42] Kennedy, S. W., Ubbelohde, A. R., and Woodward, I., Proc. Roy. Soc. (London) A**219,** 303 (1953).
[43] Kracek, F. C., J. Phys. Chem. **34,** 225 (1930).
[44] Kolomin, L. G. and Protsenko, P. I., Izv. Vyassh. Ucheb. Zaved., Fiz. **11,** 119 (1968).
[45] Meinnel, M. J. and Clinet, R., Arch. Sci. (Geneva) **10** Special 5–6, 14 (1957).
[46] Chen, A. and Chernow, F., Phys. Rev. **154,** 493 (1967).
[47] Balkanski, M. and Teng, M. K., Physics of Solid State, Ed. by S. Balakrishna, Academic Press, London (1969), p. 289.
[48] Bridgman, P. W., Proc. Amer. Acad. Arts. Sci. **51,** 581 (1916).
[49] Barth, T. F. W., Z. Physik. Chem. **B43,** 448 (1939).
[50] Davis, B. L. and Adams, L. H., J. Phys. Chem. Solids **24,** 787 (1963).
[51] Rapoport, E. and Kennedy, G. C., J. Phys. Chem. Solids **26,** 1995 (1965).
[52] Bridgman, P. W., Proc. Amer. Acad. Arts Sci. **72,** 45 (1937).
[53] Asadov, Yu. G. and Nasirov, V. I., Sov. Phys. Dokl. **15,** 324 (1970) (English Translation).
[54] Borchert, W., Z. Krist. **95,** 28 (1936).
[55] Davis, B. L. and Oshier, E. H., Amer. Minerl. **52,** 957 (1967).
[56] Fermor, J. H. and Kjekshus, A., Acta Chem. Scand. **22,** 836 (1968).
[57] Davis, B. L. and Adams, L. H., Z. Krist. **117,** 399 (1962).
[58] Janecke, E., Z. Physik. Chem. **90,** 280 (1915).
[59] Berg, L. G. and Yasnikova, T. E., Zh. Noerg. Khim. **11,** 886 (1966).
[60] Hioki, Y. and Mori, S., Natl. Tech. Rept. (Matsushite Elec. Ind. Co. Osaka) **11,** 1 (1965).
[61] Amigo, J. M., Acta Geol. Hisp. **5,** 33 (1970).
[62] Natarajan, M., Das. A. R., and Rao, C. N. R., Trans. Faraday Soc. **65,** 3081 (1969).
[63] Nolta, J. P., Schubring, N. W., and Dork, R. A., J. Chem. Phys., **42,** 508 (1965).
[64] Doucet, Y., Morabin, A., Tete, A., and Rostini, P., C.R. Acad. Sci. **261,** 3060 (1965).
[65] Gesi, K., Japan J. Appl. Phys. **6,** 781 (1967).
[66] Nurmia, M. J., Ann. Acad. Sci. Fennicae Ser. A, VI, **22,** 9 (1959).
[67] Taylor, G. W. and Lechner, B. J., J. Appl. Phys. **39,** 2372 (1968).
[68] Verzhbitskii, F. R. and Ust-Kachkintsev, V. F., Uch. Zap. Permsk. Gos. Univ. No. 111, 24 (1964).
[69] Mansingh, A. and Smith, A. M., J. Phys. D **4,** 560 (1971).
[70] Fermor, J. H. and Kjekshus, A., Acta Chem. Scand. **22,** 2054 (1968).
[71] Leong, J. T. and Emrick, R. M., J. Phys. Chem. Solids **32,** 2593 (1971).
[72] Weidenthaler, P., Collection Czech. Chem. Commun. **30,** 629 (1965).
[73] Weidenthaler, P., J. Phys. Chem. Solids **25,** 1491 (1964).
[74] Srinivasan, S., Proc. Nucl. Phys. Solid State Symp. (13th), India, **3,** 500 (1968).
[75] Karpov, S. V. and Shultin, A. A., Sov. Phys. Solid State **7,** 2761 (1966).
[76] Shultin, A. A. and Karpov, S. V., J. Phys. Chem. Solids **30,** 1981 (1969).
[77] Myasnikova, T. P. and Evseeva, R. Ya., Krist. Faz. Prev. Ed. N. N. Shirota, "Nauka i Tekhnika", Minsk, Beloruss (USSR), 41 (1971).
[78] Myasnikova, T. P. and Yatsenko, A. F., Sov. Phys. Solid State **8,** 2252 (1967).
[79] Khanna, R. K., Lingschied, J., and Decius, J. C., Spectrochim. Acta **20,** 1109 (1964).
[80] Hill, J. C. and Mohan, P. V., Ferroelectrics, **2,** 201 (1971).
[81] Shrivastava, K. N. and Venkateswarlu, P., Proc. Ind. Acad. Sci. **64A,** 275 (1966).
[82] Midorikawa, M., Ishibashi, Y., and Takagi, Y., Oyo Batsuri **37,** 30 (1968).
[83] Cleaver, B., Rhodes, E., and Ubbelohde, A. R., Proc. Roy. Soc. (London) **A276,** 453 (1963).
[84] Balkanski, M., Teng, M. K., and Nusimovici, M., Phys. Rev. **176,** 1098 (1968).
[85] Teng, M. K., J. Phys. (Paris) **31,** 771 (1970).
[86] Nusimovici, M., Ferroelec. Proc. Symp. 10th, 1966, 123 (1967).
[87] Teng, M. K., Balkanski, M., and Mourey, J. F., Solid State Commun. **9,** 465 (1971).
[88] Brugger, R. M., Bennison, R. B., Worlton, T. G., and Peterson, E. R., AEC Acc. No. 34816, Report No. IDO–17170 (vide) Nucl. Sci. Abstr. **20,** 4220 (1966).
[89] Zlavyanskii, V. T., Dokl. Akad. Nauk SSSR **58,** 1077 (1947).
[90] Tamman, G. and Bechme, W., Z. anorg. allgem. chem. **223,** 365 (1935).
[91] Salhotra, P. P., Subbarao, E. C., and Venkateswarlu, P., physica status solidi **29,** 859 (1968).
[92] Aleksandrov, K. S., Zinenko, V. I., Mikhelson, L. M., and Sirotin, Yu. I., Kristallografiya **14,** 327 (1969).
[93] Finbak, C., Hassel, O., and Strømme, L. C., Z. Physik. Chem. **B37,** 468 (1937).
[94] Kennedy, J. W., Taylor, G. F., and Patterson, J. H., physica status solidi **16,** K175 (1966).
[95] Kennedy, S. W., Nature **210,** 936 (1966).
[96] Plyushchev, V. E., Markina, I. B., and Shklover, L. P., Zh. Neorg. Khim. **1,** 1613 (1956).
[97] Arell, A. and Varteva, M., Ann. Acad. Sci. Fenn., Ser. A VI, (88), 8 (1961).
[98] Bronsted, J. N., Z. Physik. Chem. **82,** 621 (1913).
[99] Mustajoki, A., Ann. Acad. Sci. Fenn. Ser. A VI, (9), 3 (1958).
[100] Salhotra, P. P., Subbarao, E. C., and Venkateswarlu, P., physica status solidi **31,** 233 (1969).
[101] Brown, R. N. and McLaren, A. C., Acta Cryst. **15,** 974 (1962).
[102] Korhonen, U., Ann. Acad. Sci. Fenn. Ser. AI, (102), 37 (1951).
[103] Finbak, C. and Hassel, O., Z. Physik. Chem. **B35,** 25 (1937).

[104] Plyushchev, V. E., Markina, I. B., and Shklover, L. P., Dokl. Acad. Nauk SSSR **108,** 645 (1956).
[105] Finbak, C. and Hassel, O., J. Chem. Phys. **5,** 460 (1937).
[106] Bridgman, P. W., Proc. Natl. Acad. Sci. (US), **23,** 202 (1937).
[107] Rapoport, E. and Kennedy, G. C., J. Phys. Chem. Solids, **27,** 93 (1966).
[108] Kennedy, S. W., physica status solidi(a) **2,** 415 (1970).
[109] Salhotra, P. P., Subbarao, E. C., and Venkateswarlu, P., J. Phys. Soc. Japan, **27,** 621 (1968).
[110] Sato, S., Bull. Inst. Phys. Chem. Res. (Tokyo) **21,** 127 (1942).
[111] Hopkins, M. M., Rev. Sci. Instr. **35,** 1658 (1964).
[112] Freeman, E. S. and Anderson, D. A., Nature **199,** 63 (1963).
[113] Owen, W. R. and Kennard, C. H. L., Aust. J. Chem., **24,** 1295 (1971).
[114] Cerisier, P. and Guitard, J., C.R. Acad. Sci. (Paris) Ser. A+B, **268,** 1582 (1969).
[115] Mats, N. and Magneli, A., Ark. Kemi. **28,** 217 (1967).
[116] Pöyhönen, J., Sivonen, T., and Hilpela, M., Ann. Acad. Sci., Fenn. Ser. A VI, (170), 8 (1964).
[117] Salhotra, P. P., Ph.D. Thesis, Indian Institute of Technology, Kanpur (1967).
[118] Whitehouse, B. A., Ray, J. D., and Royer, J. D., J. Magn. Resonance **1,** 311 (1969).
[118a] Ferroni, E., Sabatini, A., and Orioli, P., Gazz. Chim. ital. 87, 630 (1957).
[119] Ferroni, E., Sabatini, A., and Orioli, P., Ricerca Sci. **27,** 1557 (1957).
[120] Korhonen, U., Ann. Acad. Sci. Fenn. Ser. AI, (150) 16 (1953).
[121] Cini, R. and Cocchi, M., Ricerca Sci. **27,** 2187 (1957).
[122] Riccardy, R. and Sinistri, C., Ric. Sci. Rend. Sez. **A8,** 1026 (1965).
[123] Mustajoki, A., Ann. Acad. Sci. Fenn. Ser. A VI (7), 12 (1957).
[124] Sato, S., J. Sci. Res. Inst. (Tokyo) **48,** 59 (1954).
[125] Bizouard, M., Cerisier, P. and Pantoloni, J., C.R. Acad. Sci. (Paris) Ser. C **264,** 144 (1967).
[126] Melveger, A. L., Khanna, R. K., and Lippincott, E. R., J. Chem. Phys. **52,** 2747 (1970).
[127] Shultin, A. A., and Karpov, S. V., Kristallografiya **13,** 705 (1968).

2.3. Ammonium Nitrate, NH_4NO_3

(orthorhombic, D_{2h}^{13}-Pnmm, $Z=2$, $a=4.942$ Å, $b=5.438$ Å, $c=5.745$ Å at 298 K)

Ammonium nitrate has five modifications below the melting point (442 K). The transformations between the various phases designated as I, II, III, IV, and V can be described as follows [1–6]:

$$\underset{\text{tetragonal}}{V} \overset{255\text{ K}}{\rightleftharpoons} \underset{\text{orthorhombic}}{IV} \overset{305\text{ K}}{\rightleftharpoons} \underset{\text{orthorhombic}}{III} \overset{357\text{ K}}{\rightleftharpoons} \underset{\text{tetragonal}}{II} \overset{398\text{ K}}{\rightleftharpoons} \underset{\text{cubic}}{I}$$

A metastable transition, orthorhombic (IV) $\rightleftharpoons$ tetragonal (II) at 318–323 K has also been reported by many workers [4–8] particularly when single crystals of NH_4NO_3 phase IV were grown from aqueous solution. The water present in the specimen greatly affects T_t and the velocity of this metastable transition which also depends upon the maximum temperature reached and the time of heat treatment [5]. The occurrence of this transition between modifications IV–II was found to be associated with special drying of the sample or its immersion in a nonsolvent [9, 10]. The metastable transition has been observed when the melt is cooled at a rate greater than 2 K per minute and does not show up on heating [11]. Brown and McLaren [12] from their study using various techniques showed that all the transformations were observed in the dry solid except the IV $\rightleftharpoons$ III, which was only found to take place in the presence of moisture. The structures I, II, IV, and V were found to be mutually related, forms II, IV, and V being distorted versions of form I. Form III does not bear any structural similarity to other stable forms.

Transitions in ammonium nitrate have been found to be largely time independent [13] and therefore, a well defined T_t can be specified. The presence of the metastable phases, however, gives rise to some complication in the mechanism of transformation. From x-ray analysis, the phase transitions have been interpreted as rotation-disorder transitions. Kamayashi and Yamakani [14] have reported all the transitions of NH_4NO_3 showing anomalies in the dielectric measurements and DTA. Some of these transitions were found to follow large thermal hysteresis.

Existence of a low temperature modification, VII, of ammonium nitrate below 103 K has been substantiated by microscopy, x-ray diffraction and thermal analysis [11]. NH_4NO_3 quenched at 77 K was found to consist of modifications IV and VII [11]. Specific heat measurements showed an anomaly at ~ 212 K [15] which, however, was not verified by DTA [16] and x-ray diffraction [16a]. In the low temperature rotation photographs, superstructure lines were found. Jaffray [17] repeated this work using a copper block with one hole and a copper block with two holes (NaCl as reference) and showed an anomaly between 208 and 216 K. The sample was cooled below 173 K and the measurements were made from this temperature upward

keeping a suitable warming rate. These studies indicated a new transformation at a lower temperature. It is concluded from Jaffray's results that it is to this new polymorphic transformation at 113–123 K that the modification in Raman Spectrum observed by Volkringer et al. [18] between 81 and 198 K can be attributed.

No major effect was observed on the transitions of NH_4NO_3 if small amounts of Na, Li, Ag, or Tl nitrates were present, but the transition characteristics were found to change in the presence of K, Rb or Cs-nitrates [19–21]. Addition of KNO_3 has a remarkable effect on the condition of NH_4NO_3. It decreases the density of NH_4NO_3 slightly, lowers the transition temperatures, lowers the expansion on transition, reduces the hygroscopicity and reduces the number of contact points as well as caking. It, however, does not affect the degree of hydration [22]. Effect of other impurities like $Cu(NO_3)_2$, $Mg(NO_3)_2$, $Zn(NO_3)_2$, $MnSO_4$, and $Na_2B_4O_7$ on the transitions was also studied [23]. Stabilization of the cubic phase was observed when CsCl and other halides were added. With $NaNO_2$ and $CsNO_2$, the tetragonal phase was stabilized [24]. Stabilization of the polymorphs of NH_4NO_3 as crystallized on a mica cleavage surface seemed to be a consequence of the close correspondence between the parameters of the stabilizer and those of the ammonium nitrate polymorph concerned [24]. All the mixtures from pure NH_4NO_3 to as far as 8 percent NH_4Cl were found to crystallize as homogenous mixed crystal phases of isometric (cubic) symmetry [25]. The cubic phase (I)— tetragonal (II) inversion changes from 398.5 K for pure NH_4NO_3 to 382 K for the solid solution containing 2.5 percent NH_4Cl. At 382 K, the curve of unmixing of solid solutions was encountered and along this curve, the phenomena of mixing and unmixing of solid solutions was found to take place and could be observed directly [25]. Addition of $(NH_4)_2SO_4$ affects the IV $\rightleftharpoons$ III phase transition of ammonium nitrate. With increase in sulfate content from 2 to 30 wt percent, the T_t of NH_4NO_3 increases from 310 to 311.5 K. At higher concentrations of $(NH_4)_2SO_4$, double salts are formed and there is no phase transition in the 298–323 K range [26, 27]. Nagatani [10] added octadecylamine, its nitrate or acetate to NH_4NO_3 in aqueous or cyclohexane solution in such a way that the additives precipitated on the surface of ammonium nitrate particles. DTA and x-ray diffraction showed that the effects of these additives between 0.03 and 0.3 wt percent was to extend the temperature region of stable existence of phase IV and to eliminate the transition III $\rightarrow$ IV at 305 K.

Deuterated Ammonium Nitrate, ND_4NO_3.

Hovi et al. [28] measured the deutron magnetic resonance line-widths in ND_4NO_3 between 100 and 403 K. They obtained values of 255, 308.5, 366, and 400.5 K with a maximum uncertainty of ± 2 K for the transformation temperatures of V $\rightarrow$ IV, IV $\rightarrow$ III, III $\rightarrow$ II and II $\rightarrow$ I phase transformations respectively. Niemela and Lohikainen [29] studied the spin-lattice relaxation times of deutrons in ND_4NO_3. The modification III of this substance could not be observed by them, similar to the results of Brown and McLaren [12] and Nagatani et al. [30] for dry samples of NH_4NO_3. Pöhyönen et al. [31] employed a modified DTA technique for a study of the various transformations in deuterated ammonium nitrate. The equilibrium temperature in the transformations IV $\rightleftharpoons$ III, III $\rightarrow$ II and II $\rightleftharpoons$ I were observed as, 302.8, 361.52 ± 0.06 and 400.58 ± 0.04 K, respectively. The melting point of ND_4NO_3 was found to be 1.2 K greater than that of NH_4NO_3 due to the isotope effect. In the I $\rightleftharpoons$ II transformation, thermal hysteresis was not observed as indicated earlier by a number of workers in the case of NH_4NO_3 [12, 32]. Superheating of modification II was not found to take place at the transformation II $\rightarrow$ I, while supercooling of the modification I was observed at the transformation I $\rightarrow$ II. Considerable superheating and supercooling proved characteristic of the III and II phases at the II $\rightleftharpoons$ III transformation. Small thermal hysteresis was observed during this transformation. The III $\rightleftharpoons$ IV transformation was also found to be associated with small thermal hysteresis. Modifications III and IV of ND_4NO_3 supercooled by 0.7 and 0.5 K, respectively. Consideration of the effect of deuteration on the Gibbs function of various modifications of ammonium nitrate indicated that the interaction of the NH_4^+ group with the lattice seemed to be strongest in modification III.

High Pressure Transformations: Janecke [33] found all the known transformations of NH_4NO_3 at higher pressures with his electrically heated pressure apparatus. The transitions were found only partially manifested by an uneven change in the pressure. In many cases, the change was found to be gradual over a temperature interval, and the pressure curves were rectilinear before and after the transition. The intersection of these curves corresponded to

the transition point. Phase diagrams between 273 and 473 K were determined by Bridgman [34] at pressures between 0.98 bar (1 kg cm^{-2}) and 11.77 kbar (12000 kg cm^{-2}). These show a new modification of ammonium nitrate. Recently, Rapoport and Pistorius [35] have also found a new modification VI during their study of the phase transformation of ammonium nitrate by DTA at high pressures; the pressure and temperature ranges of their study were 0–35 kbar and 223–623 K, respectively. The univarient lines of the I–VI, IV–VI, and I–IV transitions were found to meet at a triple point near 9.5 kbar and 529 K.

Leskovich [36] studied the effect of pressure on the polymorphic transformations of ammonium nitrate between stable modifications V($T < 255$ K), IV(255–305.1 K) and III(305.1–357.2 K). The average value for the increase in the volume expansion for the IV → III transition at normal pressures was found to be 6.5 percent. The temperature for the start of the IV–III transition was 316 K at a pressure of 392.24 bar. Leskovich [37] further found that modification IV does not show relaxation of pressure because of a minimum molar volume. The modification III possesses the largest molar volume of all known crystal modifications of this salt and easily transforms to modification IV at 323 K. Cerisier [38] studied the electrical conductivity of dehydrated NH_4NO_3 (polycrystalline pellet) at 1–600 bar and 355–442 K. In this temperature range, ammonium nitrate exists in two different forms. Measurements under increasing and decreasing temperatures showed a hysteresis loop related to a structural transformation.

NH_4NO_3

Measurement technique	Observations	Remarks	References
X-ray diffraction.....	Transition T_t, K (approx.) V ⇌ IV 255 IV ⇌ III 305 III ⇌ II 357 II ⇌ I 398 The structural information for various phases are: I, cubic, $Z=1$, $a=4.36$ Å at 403 K II, tetragonal, $Z=2$, $a=5.712$ Å, $c=4.924$ Å at 363 K III, orthorhombic, $Z=4$, $a=7.197$ Å, $b=7.716$ Å, $c=5.845$ Å at 323 K IV,* orthorhombic, $Z=2$, $a=5.756$ Å, $b=5.452$ Å, $c=4.931$ Å at 296 K *The room temperature structural informations given in the heading is from the NBS monograph. V, tetragonal,† $a=7.925$ Å, $c=9.820$ Å at 255 K †Also reported pseudo-hexagonal, $Z=6$, $a=5.75$ Å, $c=15.9$ Å below 255 K [2].	A metastable transition at 323 K has also been reported. In pulverized samples containing octadecylamine, its nitrate etc., complicated thermal hysteresis effects in the V–II phase change are observed. The transition involves a new reversible phase V* between V and II. T_t, V ⇌ V* is 315 K and T_t, V* ⇌ II is 318 K, both being λ-type transitions.	[1–8, 12, 39–46].
Dilatometric measurements..	The transitions have been found to be associated with considerable thermal hysteresis. T_t's by several authors do not differ by more than ±1.5 K.	Water present in the specimen greatly affects the transition temperature and velocity. In dry samples the transition often proceeds as a single crystal transformation without any appreciable change in orientation. The kinetics of the transition IV ⇌ III has been studied in detail.	[6, 7, 43, 47–50].

Measurement technique	Observations	Remarks	References
	Grinding of NH_4NO_3 increased the rate $d\alpha/dt$. Recrystallization in smaller crystals had similar effect. Lattice defects present in the surface of phase III probably belong to a higher melting modification rather than to lower melting phase IV. The volume change (ΔV) is as follows: III $\rightleftharpoons$ II -0.0148 cm^3 II $\rightleftharpoons$ I 0.0220 cm^3	The equations similar to those describing topochemical reaction were used to calculate the curves of (IV–III) transformation isotherms. $\ln(1-\alpha) = -kt^n$ and $\frac{d\alpha}{dt} = B\alpha^{2/3} = (1-\alpha)^{2/3}$, where α = degree of transformation t = time in minutes k & n are constants and $k^{1/n}$ is the reaction rate constant. For III–II transformation, α is given by $\ln(1-\alpha) = -(kt)^3$, the rate constant k rapidly increased when the temperature was further removed from T_t.	[51–58].
Differential Thermal Analysis.	The transition II $\rightleftharpoons$ III, III $\rightleftharpoons$ IV and IV $\rightleftharpoons$ V were found to show considerable hysteresis. Dry NH_4NO_3 was not found to show IV $\rightarrow$ III transition but a direct transition IV $\rightarrow$ II. The T_t shows a linear change with the logarithm of water content. heat of transitions IV–V 0.13 kcal mol^{-1} III–IV 0.42 kcal mol^{-1} II–III 0.32 kcal mol^{-1} I–II 1.03 kcal mol^{-1}	The conditions for the appearance and disappearance of the metastable transition around 318 K (II $\rightarrow$ IV) and the shift of T_t by the heat-treatment were studied in detail. The adsorbed water in the samples gave rise to a sharp large peak.	[6, 12,14, 59–62].
	Rotation disorder transition of NH_4NO_3 have been investigated.	NH_4NO_3 can be used as a temperature standard because the transition reactions are not time dependent. Metastable phases, however, make the mechanism of transition slightly complicated.	[13].
Calorimetric measurements, specific heat etc.	For a carefully dried sample, the V $\rightleftharpoons$ IV transition was found to occur at 265 K. An anomalous increase in heat capacity above 190 K was observed. The direct transition between V and II is observed in NH_4NO_3 treated with some surface active agents. For this transition $\Delta H_{tr} \sim 777.7$ cal mol^{-1} $\Delta S_{tr} \sim 2.61$ cal mol^{-1}K^{-1} The ΔH_{tr} and ΔS_{tr} for other transitions are as follows:	An analysis of the heat capacity below 100 K yielded estimates for the frequencies of torsional oscillation of NO_3^- ion and NH_4^+ ion in phase V. NH_4^+ ion is found to rotate freely in phase III in contrast to fully excited torsional oscillation in phase IV. The transition V–II is considered to occur as a combined phenomena of orientational order-disorder of the two ions NH_4^+, and NO_3^-.	[63–66].
	Transition / ΔH_{tr} cal mol^{-1} / ΔS_{tr} cal mol^{-1}K^{-1} V–IV 113.1 ± 1.5 0.430 ± 0.004 IV–III 406.3 ± 2.4 1.331 ± 0.007 III–II 322.7 ± 3.6 0.90 ± 0.01 II–I 1060 ± 7.0 2.66 ± 0.02 IV–II (metastable) 444.6 ± 5.0 1.37 ± 0.02	The small anomaly at 156 K seems to be due to the existence of a new phase VII as reported earlier [11].	

Measurement technique	Observations	Remarks	References
Dielectric constant and dispersion etc.	All the transitions have been found to show considerable hysteresis. The measurements did not show any transition near 213 K. The phase transition IV ⇌ III ⇌ II gave no significant effect on the nature of the two abnormal dielectric dispersions obtained between 25Hz and 50kHz.	Polymorphic transitions appear distinctly in capacitance-temperature curves. The dielectric constant of the phase II was found to be much higher than that of phase III, which is associated with the motion of the NO_3 groups in the unit cell.	[14, 67–70].
Ionic conductivity measurements.	Abrupt changes in conductivity were found at T_t's.		[12, 67, 71, 72].
Microscopic observations on single crystals at high temperatures.	Three different facet planes (010), (011), and (001) were studied. In the II → IV transition, the single crystal splits into two kinds of crystallites with a common c-axis but exchanged a- and b-axes. The interface between the split crystallites is parallel to the (110) plane which could be a twin plane. In the IV → II transition the split crystallites rejoin into a single phase. The resultant phase in both transitions is needle shaped. The transformations IV ⇌ III and III ⇌ II were found to reconstruct and proceed according to a mechanism of distortion and recrystallization in the presence of water vapour or drops of a saturated solution of NH_4NO_3.	The splitting during the II → IV transition occurs so as to reduce the stress due to change in the lattice constants. The II phase grows in the (230) plane of the IV phase in the IV–II transition whereas the IV phase grows in the two equivalent planes (230) and (320) of the tetragonal II phase in the reverse transition. The metastable transition IV ⇌ II proceeds according to a rearrangement mechanism. No crystals of phase III were produced from a saturated solution of NH_4NO_3 even at its optimum temperature of formation. Crystals of II and IV produced from the same solution transformed into III when given a needle shock, which indicates the necessity of crystal nuclei due to lattice distortion.	[73, 74].
Birefringence.....	The transitions were recorded by change in birefringence at T_t's.	.....	[48].
Optical studies.....	T_t's 318.3 K (II′–IV) 320.8 K (IV–II) A phase II′ of tetragonal or lower symmetry was observed as the samples were annealed in the stability range of NH_4NO_3 (III). Some optical properties of NH_4NO_3(III) were revised resulting in a positive optical sign and the optical axis angle $2V_\gamma = 86 \pm 1°$.	The orientation relations in the different phase transitions were also studied. Addition of KNO_3 lowers the II′–IV transition temperature and decreases the 2V values.	[75].
Ultraviolet spectroscopy.....	A gradual shift of absorption bands has been found to accompany the thermal expansion of the crystals. At T_t's more abrupt changes in absorption spectra have been observed. Transition / ΔV, cm³: II → III +1.77; III → II −0.64; II → I +1.04	The shifts in absorption maxima due to temperature change have been interpreted in relation to changes in the distance between cations and anions.	[32].
Density measurements.....	The III ⇌ IV transition is found to accompany gradual change of the density and occurs over a temperature interval of approx. 3 K.	.....	[76].

Measurement technique	Observations	Remarks	References
Grain size measurements.....	Change in grain size is reported during the 360 K (III $\rightleftharpoons$ II) transformation in NH_4NO_3. The number of grains per unit area increased from 2 to 36.	.....	[77].

References

[1] McLaren, A. C., Rev. Pure Appl. Chem. **12,** 54 (1962).
[2] Hendricks, S. B., Posnjak, E., and Kracek, F. C., J. Am. Chem. Soc. **54,** 2766 (1932).
[3] Early, R. G. and Lowry, T. M., J. Chem. Soc. **115,** 1387 (1919).
[4] Bowen, N. L., J. Phys. Chem. **30,** 721 (1926).
[5] Tanaka, K. and Fukuyama, I., J. Phys. Soc. Japan **8,** 428 (1953).
[6] Fukuyama, I., J. Ind. Explosives Soc. Japan **16,** 2 (1955).
[7] Shinnaka, Y., J. Phys. Soc. Japan **11,** 393 (1956).
[8] Tiemeyer, R., Z. Krist. 97, 386 (1937).
[9] Whetstone, J., Acta Cryst. **7,** 697 (1954).
[10] Nagatani, M., Kogyo Kagaku Zasshi **68,** 424 (1965).
[11] Vol'fkovich, S. I., Rubinchik, S. M., and Kozhin, V. M., Izv. Akad. Nauk SSSR, Otdel Khim. Nauk 209 (1954).
[12] Brown, R. N. and McLaren, A. C., Proc. Roy. Soc. **266,** 329 (1962).
[13] Heide, K., Z. anorg. allgem. chem. **344,** 241 (1966).
[14] Kamiyoshi, K. and Yamakami, T., Sci. Repts. Res. Inst. Tohoku Univ. Ser. A, **11,** 418 (1959).
[15] Crenshaw, J. L. and Ritter, I., Z. Physik. Chem. **B16,** 143 (1932).
[16] Klug, H. P. and Johnson, W. W., J. Am. Chem. Soc., **59,** 2061 (1937).
[16a] Amoro's Portole's, J. L., Alonso, P., and Canut, M. L., Publs. dept. crist. mineral. (Madrid) **4,** 30 (1958).
[17] Jaffray, J., Compt. Rend. **224,** 1346 (1947).
[18] Volkringer, H., Freymann, M., and Freymann, R., Compt. Rend. **208,** 1005 (1939).
[19] Straub, J. and Malotaux, R. N. M. A., Chem. Weekblad. **31,** 455 (1934).
[20] Leone, R., Schweiz. Mineral. Petrogr. Mitt. **50,** 221 (1970).
[21] Campbell, A. N. and Campbell, A. J. R., Can. J. Res. **24B,** 93 (1946).
[22] Harvey, R. J., Proc. Ann. Meet Fert. Ind. Round Table 15th Washington, D.C. 15 (1965).
[23] Ganz, S. N., Varivoda, I. Kh., Kuznetsov, I. E., Dinkevich, I. D., and Larina, L. M., Zh. Prikl. Khim. (Leningrad) **43,** 732 (1970).
[24] Hocart, R. and Sicaud, A. M., Compt. Rend. **221,** 261 (1945).
[25] Bowen, N. L., J. Phys. Chem. **30,** 726 (1926).
[26] Bowen, N. L., J. Phys. Chem. **30,** 736 (1926).
[27] Panwar, K. S. and Varma, S., Technology **6,** 151 (1969).
[28] Hovi, V., Järvinen, U., and Pyykkö, P., J. Phys. Soc. Japan **21,** 2742 (1966).
[29] Niemelä, L. and Lohikainen, T., Phys. Condens. Materie **6,** 376 (1967).
[30] Nagatani, M., Yamazoe, N., and Seiyama, T., Kogyo Kagaku Zasshi **67,** 1342 (1964).
[31] Pöyhönen, J., Nissilä, P., and Jaakkola, S., Ann. Acad. Sci. Fenn. Ser. A VI (273), 12 (1968).
[32] Cleaver, B., Rhodes, E., and Ubbelhode, A. R., Proc. Roy. Soc. **A276,** 453 (1963).
[33] Janecke, E., Z. Physik. Chem. **90,** 280 (1915).
[34] Bridgman, P. W., Proc. Amer. Acad. Arts Sci. **51,** 581 (1916); **52,** 57 (1916).
[35] Rapoport, E. and Pistorius, C. W. F. T., J. Chem. Phys. **44,** 1514 (1966).
[36] Leskovich, I. A., Dokl. Akad. Nauk SSSR **85,** 595 (1952).
[37] Leskovich, I. A., Dokl. Akad. Nauk SSSR **91,** 259 (1953).
[38] Cerisier, P., C.R. Acad. Sci. **B269,** 989 (1969).
[39] Nagatani, M., Hayama, M., Yamazoe, N., and Seiyama, T., Kogyo Kagoku Zasshi **70,** 1633 (1967).
[40] Nagatani, M., Kogyo Kagaku Zasshi **68,** 1842 (1965).
[41] Amoro's Portole's, J. L., Alonso, P., and Canut, M. L., Publs. dept. crist. mineral. (Madrid) **4,** 38 (1958).
[42] Florke, W., Z. Physik. Chem. (unterricht) **40,** 71 (1927).
[43] Behn, U., Proc. Roy. Soc. (London) **A80,** 444 (1909).
[44] Finbak, C. and Hassel, O., Z. Physik Chem. **B35,** 25 (1937).
[45] Canut, M. L., Ayllon, M., and Amoro's Portole's, J. L., Estud. Geol., Inst.-Invest. Geol. "Lucas Mallada" (Madrid) **20,** 57 (1964).
[46] Shinnaka, Y., J. Phys. Soc. Japan **14,** 1707 (1959).
[47] Sieverts, A., Z. anorg. allgem. chem. **144,** 60 (1925).
[48] Vogt. K., Physik. Z. **12,** 1129 (1912).
[49] Paulik, F., Paulik, J., and Erdey, L., Mikrochim. Acta, 894 (1966).
[50] Everett. D. H. and Watson. A. E. P., Trab. reun. inter. react. solid. (Madrid), **1,** 301 (1956) (published 1957).
[51] Wolf, F. and Scharre, W., Zesz. Nauk. Univ. Poz. (11), 3 (1967).
[52] Wolf, F. and Scharre, W., Zesz. Nauk. Univ. Poz. (11), 25 (1967).
[53] Erofeev, B. V. and Mitskevich, N. I., Zh. Fiz. Khim. **24,** 1235 (1950).
[54] Erofeev, B. V. and Mitskevich, N. I., Zh. Fiz. Khim. **26,** 848 (1952).
[55] Erofeev, B. V. and Mitskevich, N. I., Zh. Fiz. Khim. **26,** 1631 (1952).
[56] Erofeev, B. V. and Mitskevich, N. I., Sbornik Nauch. Rabot, Akad. Nauk. Beloruss, S.S.R. Inst. Khim. (5), 3 (1956).
[57] Erofeev, B. V. and Mitskevich, N. I., Zh. Fiz. Khim. **27,** 118 (1953).
[58] Bellati, M. and Finazzi, L., Attir. ist. Veneto **69,** 1151 (1910).
[59] Sowell, R. R., Karnowsky, M. M., and Waltero, C. L., J. Thermal Anal. **3,** 119 (1971).
[60] Nagatani, M. and Seiyama, T., Kogyo Kagaku Zasshi **67,** 2010 (1964).
[61] Hioki, Y. and Mori, S., Natl. Tech. Rept. (Matsushita Elec. Ind. Co. Osaka) **11,** 1 (1965).

[62] Goto, M., Asada, E., Uchida, T., and Ono, K., Yukagaku **18**, 299 (1969).
[63] Veda, R. and Ichinokawa, T., J. Phys. Soc. Japan **5**, 456 (1950).
[64] Stephenson, C. C., Bentz, D. R., and Stevenson, D. A., J. Amer. Chem. Soc. **77**, 2161 (1955).
[65] Eichenauer, W. and Liebscher, D., Z. Naturforsch. **20a**, 160 (1965).
[66] Nagatani, M., Seiyama, T., Sakiyama, M., Suga, H., and Seki, S., Bull. Chem. Soc. Japan **40**, 1833 (1967).
[67] Verzhbitskii, F. R. and Ust-Kachkintsev, V. F., Uch. Zap. Permsk. Gos. Univ. (111), 24 (1964).
[68] Makosz, J. J. and Gonsior, A., Acta Phys. Pol. **A39**, 371 (1971).
[69] Yamashita, A. and Asai, K., J. Phys. Soc. Japan **18**, 1247 (1963).
[70] Fermor, J. H. and Kjekshus, A., Acta Chem. Scand. **22**, 2054 (1968).
[71] Kamatsu, H., Rept. Inst. Sci. Technol. Univ. Tokyo **5**, 15 (1951).
[72] Srinivasan, S., Proc. Nucl. Phys. Solid State Symp. (13th), **3**, 500 (1968).
[73] Seiyama, T. and Yamazoe, N., Kogyo Kagaku Zasshi **70**, 821 (1967).
[74] Noboru, Y. and Tetsuro, S., Kogyo Kogaku Zasshi **70**, 613 (1967).
[75] De Saenz, I. M., Tessore, J. C., and Leone, R., Schvociz. Mineral. Petrogr. Mitt., **50**, 209 (1970).
[76] De Saenz, I. M., Amonini, N., and Presa, S., Z. Physik. Chem. **43**, 119 (1964).
[77] Tamman, G. and Boehme, W., Z. anorg. allgem. chem. **223**, 365 (1935).

2.4. Thallous Nitrate, $TlNO_3$

(orthorhombic, $Z=8$, $a=6.287$ Å, $b=12.31$ Åű $c=8.001$ Å at 298 K)

Ferrari et al. (1) and Hinde and Kellet [2] have reported that the room temperature structure of thallous nitrate (form III) is orthorhombic and belongs to one of the two possible space groups, D_{2h}^{16}-Pbnm or C_{2v}^{9}-Pbn2_1. The unit cell constants of the room temperature structure given by these authors agree well with those of Brown and McLaren [3] and Swanson et al. [4]. Hinde and Kellet [2] suggested that the true unit cell may be regarded as being equivalent to the stacking in the direction of the c-axis, of two smaller cells possessing the c-parameters equal to half the true value.

Thallous nitrate shows two phase transitions:

$$\underset{\text{(orthorhombic)}}{\text{III}} \underset{}{\overset{350\text{ K}}{\rightleftharpoons}} \underset{\text{(hexagonal)}}{\text{II}} \overset{416\text{ K}}{\rightleftharpoons} \underset{\text{(cubic)}}{\text{I}}$$

Phase II is hexagonal with $a=10.543$ Å, $c=7.431$ Å, sp.gr. P31m and $Z=9$ [5]. Phase I is cubic with $a=4.326$ Å at 443 K in agreement with the value reported by Finbak and Hassel [7]. Brown and McLaren [3] have also pointed out that the unit cells of phases II and I are related in the same manner as forms IV and III of $RbNO_3$. Finbak and Hassel [7] suggested that the NO_3^- ion in form I is spherically symmetrical, being in a state of free rotation. Phase transitions of thallous nitrate have been reviewed by Newns and Staveley [6] and McLaren [8], who have discussed the results from thermodynamic, electrical, magnetic, optical and crystallographic measurements.

High Pressure Transformations: Bridgman [9, 10] studied the phase diagram of thallous nitrate up to 50 kbar and 473 K and later extended the study up to 100 kbar [11]. He pointed out that the phase boundary between phases I and II has very nearly the same slope in the pressure-temperature plane as that between phases II and III of $RbNO_3$ and phases I and II of $CsNO_3$. The one atmosphere transition temperatures for the above phases are very close suggesting a similarity between the corresponding phases [12].

Measurement technique	Observations	Remarks	References
X-ray diffraction.....	T_t's, 348 and 416 K for the phase transitions III $\rightleftharpoons$ II and II $\rightleftharpoons$ I, respectively.	.....	[1–5, 8].
Dilatometric studies.....	Both the transitions are followed by increase in volume, ΔV being 0.0034 and 0.0156 of unit volume at 273 K, respectively.	.....	[13].
Direct differential calorimetry.	ΔH_{tr} for II $\rightarrow$ I transition has been observed to be 907 ± 1.5 percent cal mol^{-1}.	This value is somewhat higher than that determined by indirect methods.	[14].
Heat capacity and thermal coefficient measurements.	T_t's, 352 and 416 K (on heating) and 416 K on cooling. No sharp transformation was observed on further cooling, although there was some indication of a very sluggish transformation in 353–293 K range.	After cooling from the first heating immediate reheating again showed the transition at 352 K thereby giving a positive evidence of III $\rightarrow$ II transformation.	[8].
Heat capacity measurements	Mean heat capacities of $TlNO_3$ has been measured as a function of temperature. The molar heats between 273–373 K, can be expressed by $C_p = 10.95 + 42.66 \times 10^{-3} T$. Extrapolation to 273 K gave the specific heat C_0 at that temperature. The specific heat C_t at any temperature (t in °C) was then calculated by the equation, $C_m = (C_0 + C_t)/2$; a sudden increase in C_t was found at T_t.	The results confirm that thallous nitrate is capable of existing in 3 allotropic modifications. Free rotation of NO_3^- in $TlNO_3$ has also been confirmed by the measurements of variation of molar heat with temperature.	[15, 16].
Measurements of entropies of transition.	T_t, K: 348, 416; ΔS_{tr}, cal mol^{-1} K^{-1}: 0.7, 2.18; ΔV, % increase: 0.4, 1.4	It seems unlikely that the III $\rightarrow$ II transition in $TlNO_3$ involves orientational disorder. This is contrary to previous findings of McLaren [8].	[6, 14,17].
High pressure DTA measurements (up to 45 kbar).	Phase diagram of $TlNO_3$ has been studied up to 923 K and 40 kbar. T_t, 352 and 417 K. No DTA signals corresponding to the III $\rightarrow$ II transition could be observed possibly due to the extreme sluggishness and small latent heat. Experimental points on the II/I phase boundary can be fitted by the relation, $t(°C) = 144.6 + 7.91P - 0.062P^2$.	It is possible that orthorhombic phase (III) of $TlNO_3$ may be isostructural with $RbNO_3$–V and $CsNO_3$–II. The II $\rightleftharpoons$ III transition in $TlNO_3$ is quite sluggish just like $RbNO_3$ IV $\rightleftharpoons$ V and $CsNO_3$ II $\rightleftharpoons$ III phase transitions.	[18].
Electric conductance measurements (dc & ac conductivity.	Transition II $\rightarrow$ I was accompanied by a large increase in conductivity.	Conductivity measurements of Brown and McLaren showed a drop in the σ values at 353 K (III–II transition point). Recycling showed that the fall in conductance at this transition is probably associated with the removal of moisture and that in perfectly dry samples little or no change at this temperature may be observed.	[3, 19].
Dielectric constant and resistivity.	Small maxima occur at the high temperature transitions. A low temperature transition has also been demonstrated at 238 ± 5 K by the anomalous dependence of dielectric constant and resistivity on temperature.	.....	[20, 21].

$TlNO_3$—Continued

Measurement technique	Observations	Remarks	References
Ultraviolet spectroscopy.....	A gradual shift of absorption bands is found to accompany the thermal expansion of the crystals.	In cases where crystal-structures are known, shifts in absorption maxima due to changes in temperature have been interpreted in relation to changes in distances between cations and anions. UV absorption spectroscopy provides a sensitive means for studying various thermodynamic effects in phase transformation.	[22].
Grain size measurements....	The number of grains per unit area decreased from 2 to 1 in $TlNO_3$ at III → II transformation 345.8 K.	.....	[23].
NMR studies.....	No abrupt changes in line-width at the transition temperatures were found. Immediately above and below the melting point, the magnetic resonance line was of the order of one tenth of a gauss wide. The line-width increased very rapidly as the temperature was lowered and was too large to be observed at room temperature.	It is suggested that the low temperature line-width is determined predominantly by nuclear spin exchange taking place among the nuclear moments present.	[24].
Optical measurements.....	Single crystals grown from aqueous solution, when examined under the polarizing microscope, were found to be anisotropic. On heating the III → II transformation at ~ 353 K was observed. Form II was also found to be anisotropic. II → I transformation was observed at ~ 423 K, the crystal changing to be isotropic. On cooling, I → II transformation was observed at slightly lower temperature.	The crystals retain their external shape and also their crystallographic orientations even after being taken through four II → I → II cycles. The extinction angle was usually less definite, suggesting some randomization of orientation around a mean value.	[3].

References

[1] Ferrari, A., Cavalca, L., and Tonelli, M. G., Gazz. Chim. Ital. **80,** 199 (1950).
[2] Hinde, R. M. and Kellet, E. A., Acta Cryst. **10,** 383 (1957).
[3] Brown, R. N. and McLaren, A. C., Acta Cryst. **15,** 977 (1962).
[4] Swanson, H. E., Gilfrich, N. T., and Cook, M. I., National Bureau of Standards Circular 539, Vol. 6, p. 58 (1956).
[5] Patterson, J. H., Microscope Cryst. Front **13,** 291 (1962–63).
[6] Newns, D. M. and Staveley, L. A. K., Chem. Rev. **66,** 267 (1966).
[7] Finbak, C. and Hassel, O., Z. Phys. Chem. **B35,** 25 (1937).
[8] McLaren, A. C., Rev. Pure Appl. Chem. **12,** 54 (1962).
[9] Bridgman, P. W., Proc. Amer. Acad. Arts Sci., **51,** 581 (1916).
[10] Bridgman, P. W., Proc. Amer. Acad. Arts Sci., **72,** 45 (1937).
[11] Bridgman, P. W., Proc. Amer. Acad. Arts Sci. **76,** 1 (1945).
[12] Rapoport, E. and Kennedy, G. C., J. Phys. Chem. Solids **26,** 1995 (1965).
[13] Bellati, M. and Finazzi, L., Atti r. ist. Veneto **69,** 1151 (1910).
[14] Arell, A. and Verteva, M., ann. Acad. Sci. Fenn., Ser. A VI (98), 6 (1962).
[15] Sato, S., Bull. Inst. Phys. Chem. Research (Tokyo) **21,** 127 (1942).
[16] Sato, S., J. Sci. Res. Inst. (Tokyo) **48,** 59 (1954).
[17] Bridgman, P. W., Proc. Am. Acad. Arts Sci. **51,** 603 (1915).
[18] Rapoport, E. and Pistorius, C. W. F. T., J. Chem. Phys. **44,** 1514 (1966).
[19] Kamatsu, H., Reports Inst. Sci. Tech. Univ. Tokyo **5,** 15 (1951).
[20] Dantsiger, A. Ya., Nauchn. Konf. Aspirantov 75 (1962).
[21] Fermor, J. H. and Kjekshus, A., Acta Chem. Scand. **22,** 2054 (1968).
[22] Cleaver, B., Rhodes, E., and Ubbelohde, A. R., Proc. Roy. Soc. **A276,** 453 (1963).
[23 Tammann, G. and Boehme, W., Z. anorg. allgem. chem. **223,** 365 (1935).
[24] Rowland, T. J. and Bromberg, J. P., J. Chem. Phys., **29,** 626 (1958).

2.5. 3*d*-Transition metal nitrates

The limited information available in the literature on the phase transitions of 3*d*-transition metal nitrates is summarized below.

3 *d*-Transition metal nitrates

Substances and measurement technique	Observations	Remarks	References
Chromium (III) nitrate (hydrated), $Cr(NO_3)_3 \cdot 9H_2O$, monoclinic, $P2_1/c$, $a=13.915$ Å, $b=9.681$ Å, $c=10.983$ Å and $\beta=84°16'$ [1]			
Specific heat.....	$Cr(NO_3)_3 \cdot 9H_2O$ undergoes a second order transition at 158 K.	The transition has been attributed to the onset of partial rotation of the water molecules within the crystal.	[2].
Dielectric measurements.....	Transition at 158 K has not been found to have any observable effect on polarizability.	.....	[3].
Cobalt (II) nitrate (hydrated), $Co(NO_3)_2 \cdot 6H_2O$			
Specific heat.....	$Co(NO_3)_2 \cdot 6H_2O$ undergoes a second order transition at 158 K.	The transition has been attributed to the onset of partial rotation of the water molecules within the crystal.	[2].
Thermal analysis and dilatometry in liquid media.	Curves were obtained showing the variation in volume as a function of temperature (in the range 93 K-room temperature). After several thermal cycles, a new thermal anomaly was found accompanied by a contraction of the crystal in the 253–275 K region.	Addition of water causes thermal anomalies (heat evolution) at some definite temperatures, the extent of which depends upon the quantity of water added. The thermal anomalies when the water is absorbed was also detected even when the water of hydration was lost by dessication. When the samples were kept in diethyl-ether, the anomaly shifted from 239 to 252 K. On complete evaporation after the first thermal cycle, the transition temperature was found to shift and return to 239 K in a third thermal cycle. Immersion of the crystals in petroleum ether or toluene caused no modification in thermal curves.	[4–8].
X-ray diffraction at low temperatures.	These measurements confirm the existence of three forms I, II and III hexahydrates of cobalt nitrate. I, monoclinic, $a=15.09$ Å, $b=6.12$ Å, $c=12.67$ Å, $\beta=119°$ II, $a=12.58$ Å, $b=6.29$ Å, $c=12.24$ Å III, Structure could not be ascertained.	Crystal was found to disintegrate at 198 K transformations.	[9].
Nickel (II) nitrate (hydrated), $Ni(NO_3)_2 \cdot 6H_2O$			
triclinic $a=7.694$ Å, $b=11.916$ Å, $c=5.817$ Å, $\alpha=102.3°$ $\beta=102.4$ Å, $\gamma=105.9°$ and $Z=2$, sp.gr.$P\bar{1}$			[10].
Thermal measurements, Heat capacity etc.	$Ni(NO_3)_2 \cdot 6H_2O$ shows a second order at 150 K.	The transition is attributed to the onset of partial rotation of the water molecules within the crystal. The transition temperature is dependent on the no. of water molecules in the crystal.	[2, 11].

3 d-Transition metal nitrates—Continued

Substances and measurement technique	Observations	Remarks	References
Dielectric measurements.....	The transition at 150 K was found to be unassociated with any dielectric anomaly.	.....	[3].
Nickel (II) nitrate (hydrated), $Ni(NO_3)_2 \cdot 2H_2O$			
Heat capacity.....	It showed a sharp λ-anomaly at 4.105± 0.005 K.	The anomaly is characteristic of a transition to a magnetically ordered state at T_N.	[12].
Copper (II) nitrate, $Cu(NO_3)_2$			
Spectroscopic studies.....	Transition from phase II to phase I was observed. Infrared spectra of anhydrous unsublimed cupric nitrate samples showed that metal-nitrate vibration is lower in energy for the low temp. phase II than for the high temp. phase I.	The unsublimed sample was found to be a mixture of both forms.	[13].
Copper (II) nitrate (hydrated), $Cu(NO_3)_2 \cdot 2.5H_2O$			
Proton magnetic resonance (up to magnetic field 50kOe at temperature below 1 K).	The copper ions form pairs with an exchange interaction $-J/k$ of about 5 K. In magnetic fields around 36 kOe, the much weaker inter-pair exchange J' lead to short- and long-range order below 0.55 and 0.16 K, respectively.	The phase transformation at 0.16 K is characterized by a spontaneous component of the time averaged magnetic moment of the copper ions perpendicular to the external field and disappears below 29 and 42 kOe.	[14].
Heat capacity (Temp. range: 0.5 K–4.2 K).	In zero applied field, C_p, exhibited a Schottky anomaly having the maximum value of 0.51R at 1.82 K.	The data are quantitatively described by assuming that Cu^{+2} ions exist in this salt as isolated pairs (binary clusters) coupled by isotropic antiferromagnetic exchange with $-J/k=5.18$ K.	[15].
Magnetic susceptibility (powdered sample).	A broad maximum was found at 3.2 K; measurements down to 0.4 K suggest that χ_p vanishes as T goes to zero. The susceptibilities of needle like monoclinic crystals of this salt exhibit small nearly uniaxial anisotropy about the *b* or needle axis. The temperature variation of $\chi_{\parallel}$ and $\chi_{\perp}$ is similar to χ_p.	The behaviour is quite unlike that of a typical three dimensional antiferromagnet. There is a possibility that Cu^{+2} moments in this salt might be coupled by isotropic antiferromagnetic exchange interaction either in isolated pairs (binary clusters) or in extended linear chains.	[16].
Zinc(II) nitrate (hydrated), $ZN(NO_3)_2 \cdot 6H_2O$			
Dilatometric studies.....	When up to 0.8 extra mole of water is present in this compound, an expansion is observed after the expected contraction during the cooling cycle. If as little as 0.08 mole of water is absent from the stoichiometric 6, little or no volume change is observed during cooling and a contraction followed by an expansion. is observed during the heating cycle.	.....	[17].

[1] Kannan, K. K. and Viswamitra, M. A., Acta Cryst. **19,** 151 (1965).
[2] Vasileff, H. D. and Grayson-Smith, H., Can. J. Res., **28A,** 367 (1950).
[3] Grayson-Smith, H. and Sturrock, R. F., Can. J. Phys. **30,** 26 (1952).
[4] Pouillen, P. and Saurel, J., J. Phys. (Paris) **24,** 572 (1963).
[5] Pouillen, P. and Saurel, J., Compt. Rend. **255,** 61 (1962).
[6] Pouillen, P. and Saurel, J., Compt. Rend. **256,** 145 (1963).
[7] Pouillen, P. and Saurel, J., Compt. Rend. **255,** 269 (1962).
[8] Pouillen, P. and Saurel, J., Compt. Rend. **258,** 188 (1964).
[9] Pouillen, P., Bernard, M. J., and Massause, M., Compt. Rend. **260,** 6861 (1965).
[10] Bigoli, F., Braibanti, A., Tiripicchio, A., and Tiripicchio, C.M., Acta Cryst. **B27,** 1427 (1971).
[11] Pouillen, P. and Saurel, J., Compt. Rend. **256,** 1740 (1963).
[12] Polgar, L. G. and Friedberg, S. A., Phys. Rev. **B4,** 3110 (1971).
[13] James, W. D. and Kimber, G. M., Inorg. Nucl. Chem. Letters **5,** 609 (1969).
[14] Van Tol, M. W., Heukens, L. S. J. M., and Poulis, N. J., Phys. Rev. Lett. **27,** 739 (1971).
[15] Friedberg, S. A. and Raquet, C. A., J. Appl. Phys. **39,** 1132 (1968).
[16] Berger, L., Friedberg, S. A., and Schriempf, J. T., Phys. Rev. **132,** 1057 (1963).
[17] Pouillen, P. and Saurel, J. Compt. Rend. **256,** 3056 (1963).

2.6. Silver Nitrate, $AgNO_3$

(orthorhombic, space group: one of the four D_2^1, D_2^2, D_2^3 and D_2^4, $Z=8$, $a=6.995$ Å, $b=7.328$ Å, $c=10.118$ Å, at 299 K)

Lindley and Woodward [1] reported the unit cell dimensions to be $a=6.997$ Å, $b=7.325$ Å, $c=10.118$ Å with space group Pbca and $Z=8$. This orthorhombic phase of silver nitrate (II) transforms at 432.5 K to a rhombohedral phase I which has a hexagonal unit cell with $a=5.203\pm0.005$ Å, $c=8.522\pm0.005$ Å (space group $R\bar{3}m$) at 437 [2]. McLaren [3] has reviewed the phase transition of silver nitrate and has discussed the changes observed in crystallographic, thermodynamic, electrical and optical properties. Newns and Staveley [4] have described the II→I transition in $AgNO_3$ as a first order phase change which is followed by a volume contraction of about 1 percent [5] and an entropy change of 1.37 eu [6]. A metastable phase, III, with rhombohedral structure has also been reported to be formed on cooling $AgNO_3$I from well above 433 K [7]. Davis et al. [9] have reported the volume change at the transition around 432 K to be too sluggish to become apparent, but a marked change in slope was observed above 438 K. This result does not agree with the previous results of volume change at the transition [5, 9a] of silver nitrate as a function of temperature. On cooling a sample chilled from melt, the conductance decreased sharply at about 438 K, although such a discontinuity was not observed while reheating. Optical studies of Ubbelohde and coworkers [10, 11] show a sharp change in the absorption spectrum at T_t. Fermor and Kjekshus [12] have found that $AgNO_3$ exhibits another transition at 238 ± 5 K, which was demonstrated by an anomalous dependence of dielectric constant and resistivity on temperature.

Fischmeister [8] found that on heating polycrystalline samples of $AgNO_3$, the II→I transition takes place around 432 K. The transition was reported to involve excessive fragmentation of the crystal so that satisfactory x-ray lines could only be obtained after prolonged recrystallization near the melting point.

Mauras [13] found that the transformations II→I and I→II in silver nitrate do not occur at the same temperature. There is a difference in the transformation temperatures which is caused by the volume change accompanying the transformation. Kennedy and Schultz [14] reported that the transformations at ~ 432.4 K becomes quite sluggish on undercooling the sample to room temperature. Maziers' and Van't Hoff [7] reported that silver nitrate forms a metastable phase at 353 K on cooling. This modification can persist for hours before it changes to the stable orthorhombic form. They also found that single crystals of silver nitrate nucleated spontaneously at the transition point. A maximum superheating of 14 K was noted.

High Pressure Transformation: Janecke [15] studied the II→I transition at high pressures. Bridgman [16] studied the change in volume, latent heat of transition, difference in compressibility, thermal expansion and specific heat up to 12 kbar, which was later extended to 50 kbar [17, 17a]. Four high pressure polymorphic forms were reported. Extending the measurements up to 100 kbar did not yield new polymorphic forms [18, 18a]. Rapoport and Pistorius [19] determined the phase diagram of silver nitrate by means of DTA and volumetric methods up to 45 kbar. In addition to the four phases, metastable $AgNO_3$–V could also be obtained by suitable manipulation above 21 kbar at temperatures below 323 K. The metastable $AgNO_3$ I→V transition is reversible. $AgNO_3$–V reverts to stable $AgNO_3$–II, if left under pressure overnight. Genshaft et al. [20] measured the volume change with increasing pressure in the temperature range 73–673 K for pressures up to 40 kbar.

Measurement technique	Observations	Remarks	References
X-ray diffraction.....	T_t, 433 K. Transition from orthorhombic to rhombohedral.	Microscopic and x-ray methods establish that II → I and I → II transitions take place by formation of a seed in the crystal matrix and subsequent growth of this seed. Depending on the number of nascent crystallization centres, transitions of two types occur: (i) single crystal → single crystal type (ii) single crystal → polycrystal type. There is no mutual crystallographic link between new and matrix crystalsssssss between new and matrix crystals during the II ⇌ I transition.	[2, 3, 21].
Calorimetry.....	T_t, 432.4 K ΔH_{tv}, (approx.) 0.58 kcal mol^{-1}	Heat capacity data differ from those reported by Janz et al. [23, 24] from drop calorimeter measurements.	[6, 22–25].
Differential thermal Analysis...	Examination of the cooling curves showed that either a direct reconversion to the orthorhombic variety took place or a new metastable phase appeared below 353 K; the latter was more easily formed when the sample had been heated well above 433 K and consisted of microcrystalline powder instead of one single crystal.	Grinding the sample gives a T_t 5.5 K higher than that of the unground sample. Effect of the grinding seems to be kinetic, namely the formation of a barrier to the transition.	[7, 26, 27].
Ultraviolet spectroscopy.....	A gradual shift of absorption bands is found to accompany thermal expansion and more abrupt changes in absorption spectra are observed at transformation points from one crystal structure to another.	By means of the techniques described, ultraviolet absorption spectroscopy proves a sensitive means for studying various thermodynamic effects in phase transformations.	[11].
Change in grain size and number.	The number of grains per unit area decreased from 7 to 4 for $AgNO_3$ at 433 K.	.....	[28].
Kinetic study of $AgNO_3$ (between 243 K and 444 K).	It was found that the transformation is faster in larger crystals. The transforming crystals suffer plastic deformation and the growth rates depend on crystallographic direction. Activation energy in the temperature range 303–373 K has been found to be 21.14 kcal mol^{-1}. At higher temperatures below the equilibrium point (433 K), the apparent activation energy approaches zero. It is suggested that a different process limits the rate in this region.	The rate of I → II transformation reaches a maximum at 375 K. The peak of this rate curve is shifted to higher temperatures by addition of 0.225 atom percent of Cd^{+2} Empirical relations governing the growth have been discussed. Theory of rate process was applied by Eyring et al. [29].	[14, 29].
Low temperature dielectric and resistivity measurements (193–303 K).	An anomalous dependence of ϵ and ρ on temperature at T_t is observed.	The hysteresis suggests the existence of disorder within the room temperature phase on heating.	[12].

References

[1] Lindley, P. F. and Woodward, P., J. Chem. Soc. A 123 (1966).
[2] Stroemme, K. O., Acta Chem. Scand. **24**, 1477 (1970).
[3] McLaren, A. C., Rev. Pure Appl. Chem. **12**, 54 (1962).
[4] Newnx, D. M. and Staveley, L. A. K., Chem. Rev. **66**, 267 (1966).
[5] Bridgman, P. W., Proc. Amer. Acad. Arts Sci. **51**, 603 (1915).
[6] Arell, A., Ann. Acad. Sci. Fenn. Ser. A VI (100), 3 (1962).
[7] Mazieres, C. and vant'Hoff, J., Compt. Rend. **256**, 2620 (1963).
[8] Fischmeister, H. F., J. Inorg. Nucl. Chem. **3**, 182 (1956).
[9] Davis, W. J., Rogers, S. E., and Ubbelohde, A. R., Proc. Roy. Soc. (London), **A220**, 14 (1953).
[9a] Guinchant, M., C.R. Acad. Sci. Paris **149**, 569 (1909).
[10] Rhodes, E. and Ubbelohde, A. R., Proc. Roy. Soc. (London) **A251**, 156 (1959).
[11] Cleaver, B., Rhodes, E., and Ubbelohde, A. R., Proc. Roy. Soc. **A276**, 453 (1963).
[12] Formor, J. H. and Kjekshus, A., Acta Chem. Scand. **22**, 2054 (1968).
[13] Mauras, H., C.R. Acad. Sci. **C272**, 973 (1971).
[14] Kennedy, S. W. and Schultz, P. K., Trans. Faraday Soc. **59**, 156 (1963).
[15] Janecke, E., Z. Physik. Chem. **90**, 280 (1915).
[16] Bridgman, P. W., Proc. Amer. Acad. Arts. Sci. **51**, 581 (1916).
[17] Bridgman, P. W., Proc. Natl. Acad. Sci. **23**, 202 (1937).
[17a] Bridgman, P. W., Proc. Amer. Acad. Arts Sci. **72**, 45 (1937).
[18] Bridgman, P. W., Rev. Mod. Phys. **18**, 1 (1946).
[18a] Bridgman, P. W., Proc. Amer. Acad. Arts Sci., **76**, 1 (1945).
[19] Rapoport, E. and Pistorius, C. W. F. T., J. Chem. Phys., **44**, 1514 (1966).
[20] Genshaft, Yu. S., Livshits, L. D., and Ryabinin, Yu. N., Sov. Phys. Tech. Phys. **12**, 126 (1967).
[21] Asadov, Y. G., Sov. Phys.-Crystallography **12**, 357 (1968).
[22] Reinsborough, V. C. and Wetmore, F. E. W., Aust. J. Chem., **20**, 1 (1967).
[23] Janz, G. J., James, D. W., and Goodkin, J., J. Phys. Chem., **64**, 937 (1960).
[24] Janz, G. J. and Kelly, F. J., J. Phys. Chem. **67**, 2848 (1963).
[25] Adams, M. J. and House, J. E. (Jr.), Trans. Ill. State Acad. Sci. **63**, 83 (1970).
[26] Berg, L. G. and Yasnikova, T. E., Zh. Neorg. Khim. **11**, 886 (1966).
[27] Negishi, A. and Ozawa, T., Thermochim. Acta **2**, 89 (1971).
[28] Tamman, G. and Boehme, W., Z. anorg. allgem. chem. **223**, 365 (1935).
[29] Eyring, H., Cagle, F. W. (Jr.), and Christensen, C. J., Proc. Natl. Acad. Sci. (US), **44**, 120 (1958).

3. Carbonates

The carbonates of alkali metals, alkaline earth metals, thallium, some of the 3*d*-transition metals and silver have been reported to undergo phase transformations. Of these, the alkaline earth metal carbonates have been investigated extensively.

3.1. Alkali Metal Carbonates

Alkali metal carbonates are highly reactive even at low temperatures and undergo varying degrees of dissociation at higher temperatures. This results in contamination of specimens complicating studies of these compounds. There is not much work reported on phase transformations of these solids in the literature. Following is an account of the available information on individual carbonates.

Lithium Carbonate, Li_2CO_3, monoclinic, I2/c, $Z=4$, $a=8.11$ Å, $b=5.00$ Å, $c=6.21$ Å and $\beta=109°41'$ [1].

Reisman [2] reported a phase transformation in this compound at 683 ± 3 K from his DTA studies. In the absence of CO_2, an additional heat effect appeared at 623 K. The 683 K transformation is not affected by the 623 K heat effect which indicates that the latter is due to either a phase transformation in Li_2O or more probably to the eutectic solidification in the high carbonate region of the system Li_2O-Li_2CO_3, obtained on dissociation [3]. Semenov and Zabolotskii [3] from their DTA, electrical conductivity and gas volumetric studies show a new phase transformation in Li_2CO_3 at 439 K.

Sodium Carbonate, Na_2CO_3, monoclinic, $Z=4$, $a=8.90$ Å, $b=5.24$ Å, $c=6.04$ Å and $\beta=101.2°$ at 296 K [4].

There are two solid state phase transformations in Na_2CO_3 below melting point [4]:

III	$\xrightarrow{634\ K}$	II	$\xrightarrow{762\ K}$	I
c-centered monoclinic		*c*-centered monoclinic		primitive hexagonal

The crystal data for phases II and I are as follows: II, $Z=4$, $a=9.000$ Å, $b=5.24$ Å, $c=6.31$ Å, and $\beta=96.9°$ (713 K); I, $Z=2$, $a=9.01$ Å, $b=5.20$ Å, $c=6.50$ Å, and $\beta=90°$ (773 K). γ-β transition is gradual and $(2a+b)_\alpha=a_\beta$, $a_\alpha=b_\alpha=b_\beta$, and $c_\alpha=c_\beta$.

Dubbeldam and DeWolff [5] show that phase III is a deformed version of hexagonal phase I. Thermal measurements of Popov and Galchenko [6] show that the transition III→II is of second order with $\Delta H_{tr}\sim200$ cal mol^{-1}, while II→I is of first order with $\Delta H_{tr}\sim450$ cal mol^{-1}. Jaffray and Martin [7] however, reported that III→II transition is not accompanied by any change in latent heat or modification. Thermodynamic investigations [8] in the temperature range 15–300 K did not show any anomaly.

Potassium Carbonate, K_2CO_3, monoclinic, $a=5.658$ Å, $b=9.858$ Å, $c=6.916$ Å and $\beta=98.30°$ at 386 K [9].

Makrov and Shul'gina [10] on the basis of their DTA studies reported that K_2CO_3 undergoes transformations at 523, 703, and 898 K. Jaffray and Martin [7] found second order transitions in K_2CO_3 at 683 and 738 K accompanied with thermal hysteresis. Reisman [2] from DTA studies differentiated between the results obtained in air and carbon dioxide. He concluded that potassium carbonate undergoes only one phase transformation (at 695 K± 2 K) and that other thermal effects occurring in atmospheric conditions are due to the impurities such as KOH and KCl. Schneider and Levin [9] studied the phase transformation in this solid by x-ray, DTA and differential scanning calorimetry. They substantiated Reisman's result that K_2CO_3 undergoes one reversible transformation and that other heat effects in air must be associated with impurities. High temperature x-ray diffraction and differential scanning calorimetry [9] show T_t to be 693±5 K. Schneider and Levin [9] concluded that the monoclinic to hexagonal transformation is of second order. The crystal data for the hexagonal phase is as follows: at 698 K $a=5.705$ Å and $c=7.169$ Å.

Rubidium, Carbonate (No crystallographic data seem to be available).

Reisman's DTA studies [2] show a second order phase transformation (II → I) in Rb_2CO_3 at 576±2 K. No new heat effects were observed in the presence of air. High pressure DTA studies of Pistorius and Clark [11] showed no transition up to 40 kbar at 298 K. The I/II transition line rises with pressure to the triple point at 9 kbar, 675 K, where the I/II transition line splits up into two separate transition lines with the appearance of a new phase III. The DTA signals associated with the new transitions become somewhat smaller with increasing pressure and are not observed beyond 27 kbar. Decompression retraces the behaviour in the reverse direction.

References

[1] A.C.A. Monograph, No. 5, Ed. J.D.H. Donnay and G. Donnay, 198 (1963).

[2] Reisman, A., J. Am. Chem. Soc. **80,** 3558 (1958).

[3] Semenov, N. N. and Zabolotskii, T. V., Izv. Sibirsk. Otd. Akad. Nauk SSSR, 58 (1962).

[4] Brouns, E., Visser, J. W., and DeWolff, P. M., Acta Cryst. **17,** 614 (1964).

[5] Dubboldam, G. C. and DeWolff, P. M., Acta Cryst. (B) **25,** 2665 (1969).

[6] Popov, M. M. and Galchenko, G. L., J. Gen. Chem. (USSR) **21,** 2489 (1951).

[7] Jaffray, J. and Martin, P., J. Physiq. Rad. **14,** 553 (1953).

[8] Waterfield, C. G., Linford, R. G., Goalby, B. B., Bates, T. R., Elyard, C. A., and Staveley, L. A. K., Trans. Faraday Soc. **64,** 868 (1968).

[9] Schneider, S. J. and Levin, E. M., J. Amer. Ceramic Soc. **56,** 218 (1973).

[10] Makarov, S. Z. and Shul'gina, M. P., Izv. Akad. Nauk SSSR, Otd. Khim. Nauk (5), 691 (1940).

[11] Pistorius, C. W. F. T. and Clark, J. B., Z. Physik. Chem. (Frankfurt) **68,** 157 (1969).

3.2. Alkaline Earth Metal Carbonates

Thermal as well as pressure transformations are known in $CaCO_3$, $SrCO_3$ and $BaCO_3$. Pauling [1] has shown that the different structures of these carbonates are determined by the cation-anion radius ratio; thus, for values of 0.67 or below, the favourable structure is calcite type with a primary cation coordination of 6. $MgCO_3$ crystallizes in the calcite structure and the radius ratio in this case is 0.47. When the radius ratio is above 0.67 but below 0.85, the aragonite phase with a pseudohexagonal-orthorhombic structure (where the ligancy of cations is 9) is favoured. It is interesting that the critical value of radius ratio of 0.67 is the exact value for $CaCO_3$ which is dimorphous. Above a radius ratio of 0.85, other structures are possible just as in $RbNO_3$ or $CsNO_3$, where the primary cation coordination is likely to be 12.

Calcium carbonate, $CaCO_3$, hexagonal (calcite), $D_{3d}^6-R\bar{3}c$, $Z=6$, $a=4.989$ Å and $c=17.062$ Å at 299 K.

Other than calcite, $CaCO_3$ exists as aragonite (orthorhombic, D_{2h}^{16}-Pbnm (Pnma), $Z=4$, $a=4.959$ Å, $b=7.968$ Å and $c=5.741$ Å at 299 K) [2] and vaterite (hexagonal, $Z=12$, $a=7.16$ Å and $c=16.98$ Å at 298 K) forms [3, 4, 5]. Meyer [6] reported vaterite to have a pseudohexagonal form with space group D_{2h}^{16}-Pbnm and $Z=4$, the plane of the CO_3 group being parallel to the c-axis. Both aragonite and vaterite forms transform to the stable calcite phase on heating [7]. Preparation of aragonite and its transformation to calcite have been the subject of investigation by many workers [8]. Presence of small amounts of strontium stabilizes the aragonite phase. Attempts to prepare very pure aragonite (without traces of Sr^{+2}) have not been very successful [7, 9].

Transformation of aragonite to calcite (A → C) takes place in the range 753–773 K, the actual T_t varying with the nature and amount of impurities present [7]. The A → C transformation is irreversible at normal pressures and proceeds by a reconstruc-

tive mechanism involving a change from 6 to 9 in the primary coordination [8]. Thus, the A → C transformation is sluggish and is associated with a large energy of activation. The effect of various impurities on the enthalpy and temperature of transformation as well as on the dissociation of calcite have been reported in detail by Rao and coworkers [7]. Meyer [6] and Kamhi [5] proposed the C_s and C_{2v} symmetry, respectively, for the carbonate ion. Infrared spectroscopic investigations by Sato and Matsuda [10] as well as Sterzel [11] have confirmed the C_{2v} symmetry of the CO_3^{-2} ion as proposed by Kamhi [5].

Vaterite transforms to calcite either directly or through the aragonite phase as an intermediate [12, 13]. Transformation of vaterite takes place in the region 623–673 K with an enthalpy of ~ 200 cal mol^{-1} [6, 7]. The kinetics of the vaterite → calcite transformation have been reported by Northwood and Lewis [14]. Northwood and Lewis observed x-ray line broadening of vaterite samples which were ground; the line broadening was attributed to the existence of microstrains in the vaterite lattice.

High pressure Transformations: Calcite transforms to the aragonite phase under pressure, the aragonite phase being stable at high pressures. In addition to calcite and aragonite phases, two other phases, II and III, were discovered by Bridgman [15] under isothermal compression of ordinary calcite at room temperature. Discontinuities in the isothermal compressibility values were detected at 14 and 18 kbar corresponding to calcite → $CaCO_3$–II and $CaCO_3$–II → $CaCO_3$–III transitions, respectively. The existence of these phases was confirmed by independent powder x-ray diffraction studies of Jamieson [16] and Davis [16a], although with divergent structural inferences. According to Jamieson [16], the phases I, II, and III of $CaCO_3$ are characterised by varying degrees of orientational disorder of the carbonate ion and are related to the normal calcite structure. Davis [16a], however, doubted the anion rotation mechanism of calcite → $CaCO_3$–II transition. The results of Jamieson [16], Davis [16a] and Rapoport [17] indicate that $CaCO_3$–II is isostructural with the ferroelectric KNO_3 phase III or with the high temperature anion disordered phase of $NaNO_3$ and that $CaCO_3$–III is isostructural with the high pressure orthorhombic phase IV of KNO_3. Fong and Nicol [17a], from their Raman spectral studies, however, disagree with the above results that show isostructural relations between $CaCO_3$ and alkali metal nitrates.

Calcite, on grinding, is known to produce aragonite [18]. Leiserowitz and coworkers [18a] have reported a shock-induced calcite-aragonite transformation. Northwood and Lewis [14] have examined the effect of microstrains on the calcite → aragonite equilibrium. The transformation is initiated by the nucleation of the aragonite phase at these microstrain sites and is followed by growth of the aragonite phase. The kinetics of the calcite-aragonite pressure transformation have been studied by Davis and Adams [19] employing x-ray diffraction.

$CaCO_3$

Measurement technique	Observations	Remarks	References
x-ray diffraction.....	T_t(aragonite-calcite), 723 K.....	During the transformation the [001] direction in aragonite changes to [111] direction in calcite structure. Single crystal aragonite breaks into calcite as polycrystalline aggregate in the course of the phase transition.	[20–29].
	Vaterite changes progressively to calcite and aragonite structures during ball milling. The vaterite to calcite and/or aragonite transition is affected by air or water vapour.	The samples of vaterite during ball milling develop microstrains and this is indicated by line broadening in diffraction patterns.	[12–14, 30].
		The structure of vaterite can be described by a disordered stacking sequence of single layers of trigonal symmetry, mostly related by glide reflections, sometimes by screws parallel to the *c* axis.	
X-ray diffraction under high pressures (up to 773 K and 15 kbar).	The rates of transformation are both temperature and pressure dependent. Around 673 K, the rate of calcite-aragonite change at	Extrapolation of experimental data indicates that the transformation rate would be negligible at 298 K. Phase diagram of	[19, 31].

Measurement technique	Observations	Remarks	References
	~ 15 kbar is similar to the reverse transformation at 1 bar. E_a, 106 kcal mol^{-1} at 1 bar.	calcite-aragonite in the range 10 to 12.7 kbar and 683 to 848 K is presented.	
	Metastable forms of calcite, I, II and III are possible intermediate phases during calcite-aragonite transformation.	Aragonite is the stable form at 20 kbar and 298 K, with respect to calcite II and III. Aragonite and vaterite showed no transition up to 24.4 kbar. Calcite undergoes changes in agreement with the thermodynamic evidence that calcite II is an anion-disordered form of normal calcite.	[16, 32].
	Transition: I→II; ΔH_{tr} +10 cal mol^{-1}; ΔS_{tr} 0.032 cal mol^{-1} K^{-1}; ΔG (1, T) 46 cal mol^{-1} II→III; −381; −1.28; 438 I→aragonite; −370; −1.24; 273		
		Crystals with calcite structure in quenched assemblages are uniaxial indicating that the biaxial nature of inverted calcite is not due to pressure. Hence the constraint imposed by aragonite morphology during the quenching and inversion to calcite has been sufficient to strain the calcite structure.	[33].
Shock induced calcite.....	Implosion of pure calcite leaves only CaO as the product. If, however, 10 percent water is present in calcite, implosion gives a good yield of aragonite as detected by x-rays.	Since it is known that a combination of shear with hydrostatic pressure accelerates the rate of phase change in the direction allowed by the pressure-temperature relationship of the compressed phases, the transformation of calcite to aragonite should take place, in shock loaded calcite. The transformation may be considered to be an ionic displacement from a distorted FCC to a distorted HCP arrangement which must involve shear since it cannot be expected to result from mere compression.	
Effect of grinding calcite samples.	Aragonite is obtained in small yields for small duration of grinding. With greater periods of grinding substantial proportions of calcite are converted to aragonite. Mechanical grinding of calcite in ball mills for up to 90 hrs. yields 70 percent aragonite and 30 percent calcite in an equilibrium mixture.	The calcite-aragonite transformation may be compared to the process of 'slip' frequently observed in metal crystals. Transformation is reported to be characteristic of nucleation-growth process. The nucleus is probably formed by atomic movements produced by microstrains during grinding.	[16, 35, 35a].
Differential thermal analysis.	T_t, 660–761 K (aragonite-calcite) ΔH_{tr}, 50 cal mol^{-1} (for pure aragonite) E_a, 100 kcal mol^{-1} ΔH_{tr}, 230 cal mol^{-1} is the maximum value encountered with 1 atom percent Sr^{+2} impurity.	Effect of varying amounts of Sr^{+2} and other cations on T_t and ΔH_{tr} as well as E_a has been investigated. Smaller cations like like Li^+, Na^+, Mg^{+2}, Cd^{+2} show relatively low T_t, but E_a is unaffected except by Cd^{+2}. It is likely that cations like Na^+ or Cy^{+3} may produce some anion or cation vacancies which affect such transformations.	[7, 28, .36–39].

Measurement technique	Observations	Remarks	References
	T_t, 623–673 K (vaterite-calcite transformation) ΔH_{tr}, 200 cal mol^{-1}	.....	[7].
Kinetic study of A–C transformation.	The transformation of aragonite to calcite was accompanied by a change in crystallite size around T_t. A marked contraction in the unit cell volume of aragonite, before it got transformed to calcite, was reported.	A model based on surface nucleation and progress of the reaction by interfacial growth is found to explain satisfactorily the complete course of the transformation of aragonite to calcite.	[39a].
Dilatomatry.....	Isothermal expansion at T_t, is ~ 2.5 percent at the aragonite-calcite transformation. The transformation is always preceded by an induction period, which is affected by i) mixing of fine calcite crystals with aragonite phase ii) rapid cooling of the sample iii) atmosphere, e.g., when atmosphere is rich in CO_2, the induction period is considerably short.	Hysteresis of about 5–8 K was noticed. For samples purified by zone-refining, the hysteresis was maximum. The T_t differs slightly with the process of preparation of the sample. Speed of the transformation is proportional to time up to about 50 percent transformation for natural aragonite.	[40–44].
	Temp. range (K) / E_a (transformation) (kcal mol^{-1}) / E_a (nucleation) (kcal mol^{-1}) 639–679 / 60 / 90 683–723 / 84 / 72		
	The molar volume of vaterite decreases during its transformation to calcite or aragonite.	The kinetics of vaterite-calcite transformation is similar to that of aragonite-calcite transformation.	[41].
High pressure experiments on C–A transformation by volume change method.	The transition takes place around 4.35 kbar and at 373 K.	The effect of various impurities on the calcite-aragonite equilibrium is discussed. Aragonite is a metastable phase of $CaCO_3$ at 1 bar and 298 K.	[45–49].
Electrical conductivity at various pressures.	Equilibrium points for calcite-aragonite from conductivity experiments: T, K / P, kbar 302.1 / 3.980 311.2 / 4.130 325.6 / 4.500 350.1 / 4.800	All normal natural occurrences of aragonite must be due to metastable formation rather than equilibrium, since the geothermal gradient lies completely in the calcite field.	[50].
Refractive index measurements.	Complexly twinned calcite results from a quenched assemblage of $CaCO_3$, liquid and vapour. These inverted calcite crystals are biaxial with optic axial angles ranging from nearly 0 to 20° (for aragonite, the optic axial angle is 18°). The isogyres appear to remain just as sharp as those in a uniaxial calcite crystal, but the crystals exhibit undulose extinction. This phenomena was noted in the range 673–1073 K and 8–20 kbar.	The uniaxial crystals with calcite morphology in quenched assemblages indicate that the biaxial nature of inverted calcite is not due to pressure.	[33].
Infrared spectroscopy.....	IR absorption spectra show changes at ~ 4 kbar and is strongly suggestive of the calcite-aragonite transformation.	However, x-ray diffraction studies on unloading do not confirm this transition. The change in IR-absorption spectra may be associated with minor structural distortions in calcite.	

$CaCO_3$—Continued

Measurement technique	Observations	Remarks	References
Electron diffraction.....	The diffraction patterns showed the following orientation relation: $[\bar{1}10]_{aragonite} \parallel [\bar{1}2\bar{1}0]_{calcite}$ $[001]_{aragonite} \parallel [0001]_{calcite}$	The orientation relation suggests that the transformation is martensitic type shear being on the (001) aragonite plane.	[52].
Electron microscopy.....	Aragonite undergoes a sudden and violent transformation to calcite when heated by the electron beam.	Twins and dislocations disappear leaving a strained crystal of aragonite or occasionally calcite structure.	[28, 53].
Kinetics of aragonite to calcite transformation in solution.	The transformation proceeds by subsequent nucleation and growth of calcite on aragonite surface. E_a, 57.4 kcal mol^{-1}.	The fraction of aragonite transformed to calcite at 323–440 K is proportional to the reaction time. The E_a value is discussed in terms of a loosely hydrated calcium bicarbonate ion pair. Effect of ions like Ba^{++}, Sr^{++}, Pb^{++}, or $SO_4^{=}$ on the calcite-aragonite equilibrium is discussed.	[54–57].
	The transition from vaterite involves nucleation and growth of aragonite in vaterite.	Geologically common ions have specific effects on the transformation.	[58].
Kinetics study (by Hahn emanation).	The rate of transformation (aragonite-calcite) is quite large above 723 K at the heating rate of 6 K min^{-1}. Around 783 K the transformation is maximum. Calcite dissociates at ~1183 K at atmospheric pressures.	Results by this technique are confirmed by x-ray diffraction measurements.	[59, 60].
Ultrasonic studies (up to 38 kbar).	Longitudinal velocities decrease sharply from 5.3 km sec^{-1} at a mean pressure of 4 kbar to minimum of 4.8 km sec^{-1} at 8 kbar. Transverse velocities decrease from 3.1 to 2.9 km sec^{-1}. Bulk and rigidity moduli also show a 10 percent decrease as the minimum density increases by about 1.7 percent.	These observed changes are attributed to calcite aragonite transformation. The low and high pressure phases possibly coexist over a considerable pressure range. The maximum and minimum in the investigations have also been attributed to the formation of metastable forms of calcite viz. calcite I, II etc.	[61, 62].

Strontium carbonate, $SrCO_3$, orthorhombic, D_{2h}^{16}-Pmcn, $Z=4$, $a=5.107$ Å, $b=8.414$ Å and $c=6.029$ Å at 299 K.

Strontium carbonate undergoes a phase transition around 1200 K from the orthorhombic (aragonite-type) structure to a hexagonal (calcite-type) structure [63]. The transformation was first pointed out by Boeke [64]. In the hexagonal structure, the lattice constants are $a=5.092$ Å and $c=9.53$ Å [63]. The transformation is similar to the aragonite-calcite transition of $CaCO_3$. The ΔH_{tr} of the transition is 4.0 kcal mol^{-1} [65] typical of a first order transition. Lander [63] could not detect any other transition in $SrCO_3$ up to 1575 K in his x-ray diffraction studies. However, Baker [66] reports that under careful conditions a second endothermic transition occurs at 1690 K. This change takes place from the hexagonal to a cubic modification. The transitions in $SrCO_3$ are believed to be the result of anion-rotational disorder.

$SrCO_3$

Measurement technique	Observations	Remarks	References
x-ray diffraction.....	T_t, 1185 K (orthorhombic-hexagonal)	The transition is related to the rotational activity of the CO_3^{-2} ions	[63].
Calorimetry.....	T_t, 1197 K (orthorhombic-hexagonal); ΔH_{tr}, 4.0 kcal mol^{-1} T_t, 1690 K (hexagonal-cubic); ΔH_{tr}, 0.800 kcal mol^{-1} (calculated).	The hexagonal-cubic transition (T_t, 1690 K) was observed in an atmosphere of CO_2 (at ~ 20 bar pressure), to prevent the $SrCO_3$ decomposition. T_t is slightly reduced (by ~ 6 K) by the presence of impurity.	[65, 66].
DTA (at high pressures).....	T_t, 1203 K (orthorhombic-hexagonal) ΔH_{tr}, 4.7 kcal mol^{-1} ΔV, 1.49 ± 0.1 cm^3 mol^{-1}	Hexagonal-cubic transition was not detectable. ΔV calculated from the slope of P–T curves agrees well with the experimental data.	[67].
Hahn emanation method (coprecipitation with ThX).	T_t, 1198 K (orthorhombic-hexagonal)	Changes in crystal structure show an increase or a decrease in emanation power due to loosening of crystal structure and consequent increase in surface area and/or diffusion rate.	[59, 60, 68].

Barium carbonate, $BaCO_3$, orthorhombic, D_{2h}^{16}-Pmcn, $Z=4$, $a=5.314$ Å, $b=8.904$ Å and $c=6.430$ Å at 299 K.

Two transformations have been reported in $BaCO_3$ [63]. At 1076 K, $BaCO_3$ transforms to a calcite type hexagonal phase ($a=5.206$ Å, $c=10.55$ Å). Around 1249 K, a transition to a cubic phase takes place. These transformations are believed to be due to the onset of rotational disorder of anions. The pressure dependence of the transitions have been reported by Rapoport and Pistorius [68] employing high pressure DTA.

$BaCO_3$

Measurement technique	Observations	Remarks	References
X-ray diffraction	T_t (orthorhombic → hexagonal), 1076 K. T_t (hexagonal → cubic), 1249 K. For cubic phase, $a=6.96$ Å at 1233 K.	The transformations are discussed in terms of rotational disorder of CO_3^{-2} ions and by analogy to alkali nitrate transformations. No new phases are known above the cubic phase up to 1573 K.	[63].
Calorimetry	Transition: Orthorhombic to hexagonal (T_t, 1079 K); ΔT, K: 50; ΔH_{tr}, kcal mol^{-1}: 3.880 Transition: Hexagonal to cubic (T_t, 1241 K); ΔT, K: 20; ΔH_{tr}, kcal mol^{-1}: 0.700	.....	[65].
DTA (at high pressures)	T_t, 1072 K; ΔH_{tr}, 4.49 kcal mol^{-1}; ΔV, 1.25 ± 0.09 cm^3 mol^{-1}. T_t, 1233 K.	No new phases are known. The ΔV calculated from the slope with Clausius-Clapeyron equation agrees well with experimental values. Studies on the higher transition were subjected to limitation because of incipient decomposition of $BaCO_3$. Doubtful indications of a higher order transition in the range 673–773 were noticed.	[15, 67].
Hahn emanation (coprecipitation with ThX).	T_t, 1083 K (orthorhombic-hexagonal)	Changes in crystal structure show an increase or a decrease in emanation power due to loosening of crystal structure and consequent increase in surface area and/or diffusion rate.	[59, 60, 68].

References

[1] Pauling, L., "Nature of Chem. Bond", Cornell University (1960).
[2] "Standard x-ray Diffraction Powder Patterns", National Bureau of Standards (US) Circular 539, Vol. III, 53 (1954).
[3] McConnell, J. D. C., Min. Mag. **32**, 535 (1960).
[4] Gibson, R. E., Wyckoff, R. W. G., and Merwin, H. E., Amer. J. Sci. **10**, 325 (1925).
[5] Kamhi, S. R., Acta Cryst. **16**, 770 (1963).
[6] Meyer, H. J., Fortschr. Mineral. **38**, 186 (1960).
[7] Subba Rao, G. V., Natarajan, M., and Rao, C. N. R., J. Amer. Cer. Soc. **51**, 179 (1968).
[8] Rao, K. J. and Rao, C. N. R. in "Progress in Solid State Chemistry", Ed. H. Reiss, Vol. 4, 131 (1967).
[9] Subba Rao, M. and Yoganarasimhan, S. R., Amer. Mineral. **50**, 1489 (1965).
[10] Sato, M. and Matsuda, S., Z. Krist. **129**, 405 (1969).
[11] Sterzel, W., Z. anorg. allg. Chem. **368**, 308 (1969).
[12] Gammage, R. B. and Glasson, D. R., Chem. Ind. (London) 1466 (1963).
[13] Matsuda, S., Nemori, M., Shiroma, A., and Sato, M., Kobutsugaku Zasshi **9**, 30 (1968).
[14] Northwood, D. O. and Lewis, D., Amer. Mineral. **53**, 2089 (1968).
[15] Bridgman, P. W., Amer. J. Sci. **237**, 7 (1939).
[16] Jamieson, J. C., J. Geol. **65**, 334 (1957).
[16a] Davis, B. L., Science **145**, 489 (1964).
[17] Rapoport, E., J. Phys. Chem. Solids **27**, 1349 (1966).
[17a] Fong, M. Y. and Nicol, M., J. Chem. Phys. **54**, 579 (1971).
[18] Burns, J. H. and Bredig, M. A., J. Chem. Phys. **25**, 1281 (1956).
[18a] Leiserowitz, L., Schmidt, G. M. J., and Shamgar, A., J. Phys. Chem. Solids **27**, 1453 (1966).
[19] Davis, B. L. and Adams, L. H., J. Geophys. Res. **70**, 433 (1965).
[20] Dasgupta, D. R., Mineral. Mag. **33**, 924 (1964).
[21] Gruver, R. M., J. Amer. Cer. Soc. **33**, 171 (1950).

[22] Shoji, H., Z. Krist. **84**, 74 (1933).
[23] Kleber, W., Neues Jahrb. Mineral. Geol. Beilage Bd. **A75**, 465 (1940).
[24] Kleber, W., Neues Jahrb. Mineral. Montash 368 (1964).
[25] Shoji, H., Bull. Inst. Phys. Chem. Res. (Tokyo) **11**, 896 (1932).
[26] Rinne, F., Z. Krist. **59**, 230 (1924).
[27] Kozu, S. and Kani, K., Proc. Imp. Akad. (Tokyo) **10**, 222 (1934).
[28] de Keyser, W. L. and Dugueldre, L., Bull. Soc. Chim. Belg. **59**, 40 (1950).
[29] Metzger, W. J. and Barnard, W. M., Amer. Mineral. **53**, 295 (1968).
[30] Meyer, H. J., Z. Krist. **128**, 183 (1969).
[31] Clark, S. P., Amer. Mineral. **42**, 564 (1957).
[32] Boettcher, A. L. and Wyllie, P. J., Nature **213**, 792 (1967).
[33] Boettcher, A. L. and Wyllie, P. J., Amer. Mineral. **52**, 1527 (1967).
[34] Dachille, F. and Roy, R., "Very High Pressure Techniques", Butterworths (London) 174 (1962).
[35] Schrader, R. and Hoffmann, Br., Z. Chem. **6**, 388 (1966).
[35a] Northwood, D. O. and Lewis, D., Can. Mineral. **10**, 216 (1970).
[36] Faust, G. T., Amer. Mineral., **35**, 207 (1950).
[37] Kulesko, G. I., Vop. Mineral. Osad. Obrazov **7**, 189 (1966).
[38] Laschenko, P. N., J. Russ. Phys. Chem. Soc. **43**, 793 (1912).
[39] Laschenko, P. N., Proc. Don. Polytech. Inst. **2**, 46 (1913).
[39a] Subba Rao, M., Indian J. Chem. **11**, 280 (1973).
[40] Pruna, M., Faivre, R., and Chaudron, G., Compt. rend Akad. Sci. (Paris) **227**, 390 (1948).
[41] Pruna, M., Faivre, R., and Chaudron, G., Bull. Soc. Chim. France, D204 (1949).
[42] Chaudron, G., Mondange, H., and Pruna, M., Proc. Intern. Symp. React. Solids, Gothenberg 9 (1952).
[43] Mondange-Dufy, H., Ann. Chim. 107 (1960).
[44] Hazlewood, F. J., Rhodes, E., and Ubbelohde, A. R., Trans. Faraday Soc. **52**, 2612 (1963).
[45] Crawford, W. A. and Fufe, W. S., Science **144**, 1569 (1964).
[46] Macdonald, G. J. F., Amer. Mineral. **41**, 744 (1956).
[47] Sclar, C. B., Carrison, L. C., and Schwartz, C. M., Amer. Soc. Mech. Engr. Paper No. 62-WA-248, 7 (1962).
[48] Simmons, G. and Bell, P., Science **139**, 1197 (1963).
[49] Bridgman, P. W., Proc. Amer. Acad. Arts Sci. **72**, 45 (1937).
[50] Jamieson, J. C., J. Chem. Phys. **21**, 1385 (1953).
[51] Schock, R. N. and Katz, S., Amer. Mineral. **53**, 1910 (1968).
[52] Hiragi, Y., Kachi, S., Takada, T., and Nakanishi, N., Nippon Kagaku Zasshi **87**, 1308 (1966).
[53] Burrage, B. J. and Pitkethly, D. R., physica status Solidi. **32**, 399 (1969).
[54] Bischoff, J. L., Ambr. Mineral. **54**, 149 (1969).
[55] Brown, W. H., Fyfe, W. S., and Turner, F. J., J. Petrol. **3**, 566 (1962).
[56] Fyfe, W. S. and Bischoff, J. L., Soc. Econ. Paleont. Mineral. (Special) **13**, 3 (1965).
[57] Bischoff, J. L. and Fyfe, W. S., Amer. J. Sci. **266**, 65 (1968).
[58] Bischoff, J. L., Amer. J. Sci. **266**, 80 (1968).
[59] Zimens, K. E., Z. Physik, Chem. **B37**, 231 (1937).
[60] Zimens, K. E., Naturwiss. **25**, 429 (1937).
[61] Ahrens, T. J. and Katz, S., J. Geophys. Res. **68**, 529 (1963).
[62] Gordon, R. B. and Vaisnys, R. J., J. Geophys. Res., **69**, 4920 (1964).
[63] Lander, J. J., J. Chem. Phys. **17**, 892 (1949).
[64] Boeke, H. E., Chem. Zentr. I., 1909 (1913).
[65] Lander, J. J., J. Amer. Chem. Soc. **73**, 5794 (1951).
[66] Baker, E. H., J. Chem. Soc. 2525 (1962).
[67] Rapoport, E. and Pistorius, C. W. F. T., J. Geophys. Res. **72**, 6353 (1967).
[68] Zimens, K. E., Z. Physik. Chem. **B37**, 241 (1937).

3.3. Thallous Carbonate, Tl_2CO_3

(monoclinic, I2/m-C_{2h}^3, $Z=4$, $a=7.55\pm0.02$ Å, $b=5.38\pm0.02$ Å, $c=10.58\pm0.02$ Å and $\beta=94°47'$[1])

Vorländer et al. [2] reported a single transition at 501 K. Tranquard et al. [3], however, showed that this transition occurs only when commercial material is used. Tl_2CO_3 purified by fractional crystallization is reported to show two new transitions at 473 and 536 K instead of the above phase transition [3]. These transitions between the phases III → II and II → I, were also confirmed by Pistorius and Clark [4] at transition temperatures 485.5 ± 2 and 533.5 ± 1 K, respectively.

High Pressure Transitions: Pistorius and Clark [4] failed to detect any high pressure transformation at 293 K up to 44 kbar. In their phase diagram studies, Pistorius and Clark [4] found that the II/I transition line falls with pressure to the I/III/II triple point at 3.4 kbar, 525 K. The resulting III/I transition slowly rises with pressure, passes through a broad maximum at 18.7 kbar, 536.8 K and then falls with increase of pressure. The III/I transition terminates at a triple point I/IV/III at 29 kbar, 532 K. A weak DTA signal observed at 34.9 kbar, 478 K is attributed to the III/IV phase transition, IV being a high pressure phase. The IV/I transition line rises with pressure and terminates at a triple point I/V/IV at 35.1 kbar, 501 K. The IV/V transition point was ascertained only be a considerable increase in slope at this point. Phase V is also a high pressure phase. The DTA signals associated with the IV/I and V/I transitions seem to be very similar to those associated with the III/I transition.

References

[1] Mitchell, R. S., Z. Krist. **123**, 399 (1966).
[2] Vorländer, D., Hollatz, J., and Fischer, J., Ber. **65**, 536 (1932).
[3] Tranquard, A., Lacassagne, C., Boinon, M., Capella, L., Cohen-Adad, R., Compt. rend. Acad. Sci., **264**, 1111 (1967).
[4] Pistorius, C. W. F. T. and Clark, J. B., Z. Physik. Chem. **68**, 157 (1969).

3.4. 3*d* Transition Metal Carbonates

Heat capacity measurements in the temperature range 1.6–80 K [1, 2] revealed that carbonates of manganese, iron, cobalt, and nickel show antiferromagnetic to paramagnetic transitions at 29.5, 30.6, 17 and 22.2 K, respectively. Measurements in the temperature range 70–300 K did not show any anomaly in these carbonates except in $CoCO_3$ which shows an anomaly due to the sorbed water [3]. Crystal structure for all these rhombohedral carbonates are tabulated by Graf [4].

3*d* Transition metal carbonates

Substances and measurement technique	Observations	Remarks	References
Manganese carbonate, $MnCO_3$, calcite type, $D^6_{3d}-R\bar{3}c$, $Z=2$ (rhomboheral cell, and $Z=6$ (hexagonal cell), $a=4.777$ Å and $c=15.67$ Å at 298 K			
Heat capacity (Temperature range: 1.6–80 K).	An antiferromagnetic-paramagnetic transition at 29.5 K is shown by a heat capacity anomaly. At liquid helium temperature the heat capacity obeys the law $C_M=aT^3$, where $a=18.0\pm0\cdot7\times10^{-4}$ J mol^{-1} K^{-4}	Excitation of the second branch of the spin wave spectrum is observed at temperature close to $T_N/10$ (T_N, 32.4 K). The results provide an experimental confirmation of the spin wave theory.	[1, 2]'
(Temperature range: 70–300 K).	No anomaly was observed. A continuous increase of heat capacity with temperature was found. The total entropy, consisting of the lattice and magnetic parts was also determined.	The entropy of magnetic ordering constitutes 14.7 percent of the total entropy. The earlier results of Anderson [5] differ from those of Kostryukov and Kalinkina [3] possibly due to the nature and quantity of impurities.	[6].
Magnetic measurements.....	Magnetic susceptibility was found to increase abruptly below T_C, 31.5 K and to vary considerably with the field.	The observed anomalies are interpreted by postulating that below T_C, $MnCO_3$ goes over to an antiferromagnetic state in which the moments of the sublattices do not fully compensate each other.	[3].
Iron carbonate, $FeCO_3$, rhombohedral (calcite type), $a=4.6887$ Å, $c=15.373$ Å [4]			
Heat capacity (Temperature range: 1.6–70 *K*).	Transformation at 30.6 K is associated with change from antiferromagnetic to paramagnetic state. Nuclear heat capacity has not been observed for $FeCO_3$ showing that Fe has zero magnetic moment.	In $FeCO_3$ the spins are parallel to the principal axis so that the magnetic heat capacity should be practically nonexistent at low temperatures.	[1].
(Temperature range: 70–300 K).....	No maximum is observed in this range. The total entropy of $FeCO_3$ comprises of lattice and magnetic contributions. The latter is 10.6 percent of the lattice entropy. The entropy of magnetic ordering constitutes 13.9 percent of the total entropy.		[3].

3*d* Transition metal carbonates—Continued

Substances and measurement technique	Observations	Remarks	References
Cobalt carbonate, $CoCO_3$, rhombohedral (calcite type), $R\bar{3}c$, $Z=6$, $a=4.659$ Å and $c=14.957$ Å at 299 K.			
Heat capacity (Temperature range: 1.6–70 K).	Transformation at 17 K is associated with a change from antiferromagnetic to paramagnetic state. At liquid helium temperature, the magnetic heat capacity obeys the law $C_M=aT^3$, where $a=13.5\times10^{-4}$ J · mol^{-1} K^{-4}.	The results agree with those given by magnetic measurements. Excitation of the second branch of the spin-wave spectrum is observed at temperature close to $T_N/3$.	[1].
(Temperature range: 70–300 K)....	Maxima found at 270 K, is attributed to the sorbed water.		[3].
	The total entropy is comprised of the lattice and magnetic contributions. The magnetic contribution for $CoCO_3$ is 8.3 percent of the lattice entropy.	At 298.15 K, the entropy of magnetic ordering contributes 13.0 percent of the total entropy.	
Magnetic measurements.....	Magnetic susceptibility increases abruptly below T_C, 17.5 K and varies considerably with field.	It is postulated that below T_C, the substance goes over to an antiferromagnetic state in which the moment of the sublattices do not fully compensate each other.	[6].
Nickel carbonate, $NiCO_3$, rhombohedral (calcite type), $D_{3d}^6-R\bar{3}c$, $Z=6$, for hexagonal unit cell, $a=4.609$ Å and $c=14.737$ Å at 298 K.			
Heat capacity (Temperature range: 1.6–70 K).	The transition at 22.2 K is associated with a change from antiferromagnetic to paramagnetic state. At liquid helium temperature, the magnetic heat capacity obeys the law $C_M=aT^3$, where $a=15.3\times10^{-4}$ J mol^{-1} K^{-4}.	The results agree well with those obtained from magnetic measurements.	[1].
(Temperature range: 70–300 K)...	No anomaly is obtained in this temperature range. The entropy of magnetic ordering was found to constitute 10.6 percent of the total entropy.		[3].
Magnetic measurements.....	Between 60 and 290 K the Curie-Weiss relation represents the temperature dependence of the susceptibility of nickel carbonate (both green as well as yellow modifications). The proportionality of the magnetization with the field disappears at 40 K and the material becomes ferromagnetic at 4 K.	.....	[7].

References

[1] Kalinkina, I. N., Sov. Phys. JETP **16,** 1432 (1963).
[2] Borovik-Romanov, A. S. and Kalinkina, I. N., Sov. Phys. JETP **14,** 1205 (1962).
[3] Kostryukov, V. N. and Kalinkina, I. N., Russ. J. Phys. Chem. **38,** 422 (1964).
[4] Graf, D. L., Am. Mineral. **46,** 1283 (1961).
[5] Anderson, C. T., J. Am. Chem. Soc. **56,** 849 (1934).
[6] Borovik-Romanov, A. S. and Orlova, M. P., Sov. Phys. JETP **4,** 531 (1957).
[7] Bizette, H. and Tsai, B., Compt. Rend. **241,** 546 (1955).

3.5. Silver Carbonate, Ag_2CO_3

(monoclinic, C_2^2–$P2_1$, $Z=2$, $a=4.836$ Å, $b=9.555$ Å, $c=3.235$ Å and $\beta=92.64°$ at 298 K)

Ag_2CO_3

Measurement technique	Observations	Remarks	References
X-ray diffraction with impure samples.	With the ratio of dopant Y(III) and Gd(III) to Ag, $n \geq 0.005$ a new orthorhombic crystal structure is reported with $a=13.94$ Å, $b=5.97$ Å, $c=5.30$ Å.	.....	[1].
Heat capacity (room temperature – 453 K).	A rapid increase in the heat capacity was observed above 423 K.	The anomaly is possibly due to the dissociation of the sample.	[2].
Differential thermal analysis	Two endotherms, first at 458 K and the second above 500 K were found. A small exotherm was also detected.	The first is attributed to a reversible transition and the second to the dissociation. The exotherm is attributed to the annealing out of defects in Ag_2O.	[3–5].
Differential scanning calorimetry (with the sample sealed in CO_2 atmosphere to prevent decomposition).	Two reversible endotherms in the temperature range 440–475 K were found. The first also observed previously [3] has ΔH_{tr}, 730 ± 80 cal mol^{-1} and the second found only in this work has ΔH_{tr}, 473 ± 30 cal mol^{-1}.	.....	[6].
EPR studies of impure samples.	EPR studies on γ-irradiated Y(III)-Doped Ag_2CO_3 also indicate the presence of a new crystal structure. The same crystal structure is thermally attained in undoped Ag_2CO_3 at approximatly 423 K under an atmosphere of CO_2.	The results agree well with x-ray diffraction studies.	[1].

References

[1] Ashford, N. A. and Snelson, A., J. Chem. Phys. **51**, 532 (1969).

[2] Kobayashi, K., Science Repts. Tohoku Univ. **35**, 283 (1952).

[3] Leyko, J. and Maciejewski, M., Bull. Acad. Pol. Sci. **12**, 273 (1964).

[4] Calbertson, W. J. (Jr.), Rept. No. AMRL-TR-64-119, Denver Res. Inst. 6570th Aerospace Med. Res. Labs., Wright-Patterson, AFB, Ohio, Dec. 1964.

[5] Rao, C. N. R., Yoganarasimhan, S. R., and Lewis, M. P., Can. J. Chem. **38**, 2359 (1960).

[6] Wyderen, T., Aust. J. Chem. **20**, 2751 (1967).